Decentralized Dynamic Matching: A Carpooling Platform*

Tracy Xiao Liu† Tsinghua University

Zhixi Wan‡ University of Hong Kong

Chenyu Yang§ University of Maryland

November 5, 2024

Abstract

We study decentralized dynamic matching using data from a large carpooling platform. The matching is between commuting drivers and passengers: drivers search for passengers with similar routes and departure times, while passengers wait to be matched. Both drivers and passengers can stop waiting and leave the platform at any time. To understand the efficiency of the market, we estimate a dynamic model of matching and simulate counterfactual matching policies. We find that policies reducing unmatched exits can significantly increase the number of matches.

Keywords: market design, dynamic matching market, carpooling platform, two-sided market

JEL: C73, D47, D83, L92, R40

1 Introduction

How should matching be organized in a designed market? In some markets, participants report their preferences and centralized algorithms create binding matches. A prime example is the placement of medical students in US residency programs. In contrast, online platforms are largely decentralized. On Uber or Lyft, a driver can accept or reject rides offered by the platform. On Airbnb, a host can accept or reject booking requests by guests. On a freelance website, a client chooses from a list of task providers. A main reason for the decentralized approach is that users of online platforms possess substantial private preference information. They may not wish to disclose this information due to privacy concerns (Goldfarb and Que, 2023), or disclosure is costly when matches need to happen

*We thank seminar and conference participants at the AEA, APIOC, Boston College, DOJ, IIOC, INFORMS, Maryland, Michigan, NASMES, NBER Market Design meeting, NBER Summer Institute (IO and Digitization), SICS, SITE, SUFE IO Conference, Rochester and Western Ontario for valuable insights and comments. We thank Sueyoul Kim and Shu Wang for excellent research assistance. Tracy Xiao Liu gratefully acknowledges financial support by the National Natural Science Foundation of China (72222005, 72342032) and Tsinghua University (No. 2022Z04W01032). Chenyu Yang acknowledges the University of Maryland supercomputing resources (http://hpcc.umd.edu) made available for conducting the research reported in this paper. The paper was previously circulated under the title "The Efficiency of A Dynamic Decentralized Two-Sided Matching Market".

†School of Economics and Management, Tsinghua University; liuxiao@sem.tsinghua.edu.cn

‡Faculty of Business and Economics, University of Hong Kong; zhixiwan@hku.hk

§Department of Economics, University of Maryland; cyang111@umd.edu

quickly. In such environments, centralized algorithms based only on information reported by agents may create undesirable matches and cause excessive rejections. Therefore it is important to identify efficient matching policies for decentralized markets that operate with limited user information.

We analyze decentralized dynamic matching using data from a large commuter carpooling platform in China, which facilitated over 130 million rides in 2023. We focus on a period on late afternoons of 20 week days in one of China's 20 largest cities. The matching works as follows. A passenger sends a request that specifies her route (origin and destination) and trip departure time. A commuting driver also reports her route and departure time to the platform, which then shows the driver a list of passengers as potential matches based on trip similarities. The driver forms a match by choosing a passenger. After the match, the driver meets the passenger at the passenger's location by the passenger's departure time to start the trip. Unmatched drivers and passengers can stop searching and leave the platform at any time. Fares are based only on the distances of the passenger trips, and because they are 50% less than taxi or ride-hailing fares, drivers on this platform are almost all commuters looking to share their ride.[1]

This decentralized design does not always produce the socially optimal matching outcome. Given the possibility that a better match will arise, drivers may choose not to match with a passenger when it would be efficient, because drivers cannot fully capture passenger surplus with distance-based fares. As a result, some passengers are left unmatched and ultimately leave the market. The welfare effect of forgoing these matches depends on agent preferences for matches and waiting costs. We illustrate how strategic waiting causes inefficiency in a simple model.

Our data provide suggestive evidence consistent with driver strategic waiting. We show that, consistent with falling waiting values, drivers who are closer to departure times are more likely to leave or match. We also show that this effect is not caused by a driver heterogeneity, where drivers who arrive closer to their departure times are more impatient. Our interviews with drivers further support these findings.

To empirically analyze the efficiency of the carpooling market, we formulate and estimate a dynamic structural model of matching. In the model, drivers decide whether to match with a passenger, wait, or leave the market without a match by comparing the value of the match, the expected value of waiting and the value of an outside option. The expected value of waiting is based on the driver's waiting cost and the equilibrium distribution of passengers. On the other side, a passenger forms a belief about the average match rate and sets an optimal leaving time. The passenger would cancel her ride request and leave the market if she is not matched by the optimal leaving time. We define a tractable equilibrium for the matching market.

Next, we estimate this model using data from the platform. We estimate the driver model in a two-step approach. In the first step, we use data on driver choices, variations in choice sets and arrival times to estimate driver preferences for matches and values of waiting. In the second step, we invert the waiting costs from the value functions. We also estimate the passenger model in two steps. We first estimate passenger beliefs about match rates and then match preferences and waiting costs.

[1] A similar service is BlaBlaCar that operates in Europe and Latin America. To target commuting drivers and discourage professional drivers, the pricing is similarly based on trip distances and material costs (such as fuels) incurred by drivers to ensure that the drivers do not make a profit (BlaBlaCar, 2024).

Using the estimated model, we first quantify the effects of driver strategic waiting on total surplus. Based on the estimated driver preferences for matches and waiting costs, we solve for the (non-equilibrium) driver waiting values maximizing the total surplus while allowing passengers to endogenously respond to the counterfactual driver strategies. The solution shows that if drivers were to lower values of waiting, the average surplus per user (across drivers and passengers) could increase by \$0.01 (2018 USD), and the number of matches would increase by 0.23%. The result suggests that, although strategic waiting causes some passengers to leave unmatched, the overall impact is small.

Different from the first simulation, which holds the decentralized matching policy fixed, our next simulations consider alternative matching policies. Specifically, these policies can potentially create more surplus or matches by changing not only the decisions to wait, but also the decisions to leave. We consider matching policies inspired by optimal algorithms in centralized matching markets. In particular, Akbarpour, Li and Gharan (2020) theoretically study centralized dynamic matching, where the platform has full knowledge of agent preferences and agents leave at exogenous times. They compare a greedy algorithm with a patient algorithm. A greedy algorithm attempts to match agents as soon as they arrive. A patient algorithm additionally requires the platform to know agent leaving times and attempts to make matches just before an agent leaves. They show that the patient algorithm maintains a thicker market and makes more matches. Furthermore, both algorithms perform better than others in large markets (Ashlagi, Nikzad and Strack, 2023). However, a direct implementation of such algorithms requires detailed knowledge of agent preferences, which may be infeasible for online platforms. Agents also leave endogenously in a decentralized market.

Therefore, we consider alternative policies that are more feasible in decentralized markets. Under our greedy policy, an arriving driver has to choose a passenger or leave immediately. Intuitively, this policy eliminates driver strategic waiting and increase the matching probability, but it also significantly reduces the number of drivers available for matching with a passenger. We find that the increase in the matching probability largely offsets the effects of fewer waiting drivers. Consequently, the number of matches increases by 0.2%, although both the driver and passenger surpluses fall. In particular, despite producing more matches, the policy matches more short trips in the downtown area, and the total revenue also falls slightly.

Our modified patient policy, like the patient algorithm for the centralized market, uses the information on the trip departure times. Under this policy, the platform requires an arriving driver to choose a passenger, leave immediately, or commit to continuing to search until her trip departure time. A driver subject to the commitment must either match with a passenger or wait. The driver can leave unmatched only when she reaches the departure time. Similarly, an arriving passenger can choose whether to leave immediately or commit to waiting till her departure time. The key motivation is that, although the platform cannot predict the precise time of unmatched exits from the market, there may be net gains to reducing such exits. The tradeoff is that fewer agents may participate in matching.

The effects of the patient policy are large. The number of matches increases by 22.26% relative to the decentralized market. Driver surplus decreases and passenger surplus increases, resulting in a net loss of total surplus. Banning unmatched exits increases matching probability, but market thickness

still decreases: the shares of agents who wait after arrival (thus agreeing to the commitment) fall more proportionally than the increase in waiting time. We also decompose the effects of the patient policy. We find that a driver-only patient policy achieves 92% of the increase in the number of matches under the full policy.

Since our decomposition result shows that drivers are more responsive to the patient policy, we next focus on adjusting driver behaviors by combining the greedy and patient policies. A hybrid policy takes the following form: a search deadline is set at t minutes before the trip departure time, and a driver must continue to search until the deadline unless she matches with a passenger; the driver reaching the deadline must leave immediately. A deadline maximizing the total surplus achieves a net surplus increase and a 5.54% gain in the number of matches. The driver surplus still falls, but the loss is more than overcome by the increase in passenger surplus.

Literature Review and Contributions

First, we contribute to the literature of dynamic matching. The market design literature studying the optimality of dynamic matching markets has theoretically explored the trade–offs between waiting time, number of matches and match quality in centralized matching markets (Ashlagi, Burq, Jaillet and Manshadi, 2019; Baccara, Lee and Yariv, 2020; Akbarpour, Li and Gharan, 2020; Loertscher, Muir and Taylor, 2022; Doval, 2022; Ashlagi, Nikzad and Strack, 2023). Our counterfactual matching policies adapt near-optimal algorithms in centralized matching markets for decentralized markets and assess their performance.

We also add to the growing empirical literature on market design (Agarwal and Budish, 2021), especially the study of dynamic allocation mechanisms in the absence of money. Prior studies include the allocation of deceased donors' kidneys (Agarwal, Ashlagi, Rees, Somaini and Waldinger, 2021), public housing assistance (Waldinger, 2021), and bear-hunting licenses (Reeling and Verdier, 2021). These studies feature agents that strategically decide whether to accept an object. We focus on a two-sided matching market where both sides of agents make dynamic and strategic decisions.[2]

In the transportation industry, a number of papers use dynamic models to study the taxi market (Lagos, 2003; Frechette, Lizzeri and Salz, 2019; Buchholz, 2022), ride-hailing platforms (Shapiro, 2018; Bian, 2020; Castillo, 2020; Rosaia, 2020; Gaineddenova, 2022) and dry bulk shipping (Brancaccio, Kalouptsidi and Papageorgiou, 2020; Brancaccio, Kalouptsidi, Papageorgiou and Rosaia, 2023). We depart from the common empirical contexts where professional drivers or shippers are matched with customers. In many of these markets, search frictions increase market thickness, but thickness causes congestion and reduces market efficiency. In contrast, the defining feature of our market is that drivers can discriminantly choose from all waiting passengers. This feature leads to a cream-skimming

[2]Our paper is also related to empirical studies of peer-to-peer platforms (Einav, Farronato and Levin, 2016). Some examples include estimating matching on an online dating website (Hitsch, Hortaçsu and Ariely, 2010), the heterogeneous competitive effects of Airbnb (Farronato and Fradkin, 2022), and the determinants of a platform's growth (Cullen and Farronato, 2020). In addition, a number of papers study how search strategies respond to experimental variations in information on market thickness (Bimpikis, Elmaghraby, Moon and Zhang, 2020; Li and Netessine, 2020; Fong, 2024). More broadly, there is a large literature studying market design using experimental methods (Roth, 2016; Chen, Cramton, List and Ockenfels, 2021; Chen, 2023). Finally, our paper is related to the large literature on two-sided markets (Rysman, 2009; Jullien, Pavan and Rysman, 2021).

incentive (Romanyuk and Smolin, 2019) and a different form of market failure.

Road Map We first highlight potential inefficiencies in a decentralized matching market using a two-period model in Section 2. In Section 3, we describe the setting and our data. Section 4 presents the empirical model. We discuss the identification and estimation of the driver and passenger decision models in Sections 5 and 6. Section 7 analyzes market efficiency and compares the equilibrium effects of various market designs, and we conclude in Section 8.

2 An Illustrative Model of Dynamic Matching in Two Periods

We first describe a simple matching model in two periods. There are two drivers $\{a, b\}$ and two passengers $\{1, 2\}$. An agent exogenously enters the market in the first or second period with probability p and $1 - p$. The entry is independent across agents. The matching in a decentralized market occurs in the following order:

1. Entry times are realized and observed by all agents.
2. The first period starts. Agents whose entry time is the first period enter the market.
   (a) Drivers move first. If no driver enters, the game proceeds to (b). If both drivers are in the market, the nature randomly picks one driver to move first with equal probability. The order of moves is observed by all agents. A moving driver decides whether to match with a passenger (if any passenger is present), wait or leave the platform unmatched. Matched drivers and passengers leave the market.
   (b) Any remaining passenger decides whether to wait or leave the market.
3. The second period starts. Drivers and passengers that did not enter in period 1 now enter the market, and steps 2(a)-(b) repeat.
4. All unmatched agents leave the market at the end of the second period.

To highlight the potential inefficiency, we assume that both drivers prefer passenger 1 to passenger 2, but their preferences for passenger 2 and leaving unmatched differ. Specifically, we use $u_{k\ell}$ to denote the match value to driver $k \in \{a, b\}$ when she is matched with a passenger $\ell \in \{1, 2\}$. We assume the value of leaving unmatched to be 0, and the preferences satisfy

$$u_{a1} > u_{a2} > 0$$

$$u_{b1} > 0 > u_{b2}.$$

Consistent with our empirical context, any driver matching with a passenger will complete the passenger's request, and therefore passengers do not have preferences over the identities of the matching driver. We assume that the value of the match for a passenger is v and the value of leaving unmatched is $0 < v$. In addition, drivers and passengers that decide to wait in period 1 incur a waiting cost c. The matching values and waiting costs are public information.

Decentralized Market

Suppose that driver a and passenger 2 enter in the first period, and driver b and passenger 1 enter in the second period.[3] We further assume that driver a has a strong preference for passenger 1, i.e., $0.5 \cdot u_{a1} - c > u_{a2}$, and passengers have a weak preference for being matched, i.e., $0.5v < c$.

We solve for the agent equilibrium choices by backward induction. In the subgame perfect Nash equilibrium, driver a does not match with passenger 2, because the driver's value of waiting is greater than the match value. The passenger then leaves the market without match. In the second period, either driver a or b matches with passenger 1, depending on nature's choice. The number of matches is 1, and the expected total surplus is $W = 0.5u_{a1} + 0.5u_{b1} + v - c$.

In this case, driver a's strategic waiting decreases the number of matches. If driver a were to lower the expected value of waiting below u_{a2}, she would match with passenger 2 in the first period, and the driver b would match with passenger 1 in the second period. The total number of matches would increase to 2.

Furthermore, strategic waiting can cause inefficiency. The total surplus is $\widetilde{W} = u_{a2} + u_{b1} + 2v$ if driver a's waiting value is below u_{a2}. When u_{b1} is sufficiently high, $\widetilde{W} > W$. In this case, the outcome where a matches with passenger 2 and b matches with passenger 1 is also the socially optimal assignment.

Greedy and Patient Policies

Under the **greedy** policy, driver a must either match with a passenger or leave by the end of period 1. This policy produces the same outcome as when we reduce strategic waiting in the above.

We next consider the **patient** policy. For simplicity, we assume that agents arrive exogenously and have agreed to not leave without a match in period 1.[4] More specifically, the policy requires driver 1 to either make a match in period 1 or wait till period 2. An unmatched passenger 2 must also wait till the second period. We show that the expected number of matches increases to 1.5 under the patient policy. In the first period, driver a still prefers waiting to matching, and passenger 2 now is forced to wait. In the second period, driver a moves first with probability 0.5 and matches with passenger 1. No other matches occur because driver b prefers leaving to matching with passenger 2. Then the total number of matches is 1. Alternatively, driver b moves first with probability 0.5 to match with passenger 1, and driver a matches with passenger 2, producing 2 matches.

Similar to the greedy policy, the welfare effect of the patient policy depends on agent preferences. The expected total surplus under the patient policy is

$$W^{\text{patient}} = 0.5\left(u_{a1} + v\right) + 0.5\left(u_{a2} + u_{b1} + 2v\right) - 2c.$$

Given that $W^{\text{patient}} - W = 0.5v - c + 0.5u_{a2}$, the patient policy improves welfare if u_{a2} is sufficiently high.

[3] This scenario occurs with probability $p^2\left(1-p\right)^2$.

[4] To endogenize the participation decision, we could consider a three-period model. Agent arrival times are randomly distributed across three periods, and unmatched agents at the end of the first period decide whether to commit to searching and waiting or leave at the end of the first period.

Relations to Our Empirical Context

As we will see in Section 3.2, a large number of driver and passenger trips in our data originate or end in a small downtown area. A driver going to or from this area (a "downtown driver") is similar to the driver a, who may see many passengers with similar routes. A non-downtown driver is more like a driver b that sees fewer passengers with similar routes, but this driver's preferred route may overlap with a downtown driver's. Therefore a greedy policy can shift matches towards downtown drivers because it is more likely for them to find potential matches upon arrival. Whether the policy can increase surplus depends on the surplus increase of downtown passengers compared with others' surplus loss. The effects of the patient policy are more nuanced. Under this policy, high-waiting-cost drivers are less likely to wait, but drivers who agree to wait are more likely to form matches. The net effect depends on whether the increase in the matching probability offsets the decrease in participation.

3 Background and Data

3.1 Matching on the Carpooling Platform

Information Reported to the Platform The carpooling platform operates without a centralized dispatch system. A prospective passenger sends a ride request to the platform, where waiting drivers decide whether to choose the request. The passenger request specifies the origin, destination, and departure time. The departure time indicates the time when the passenger wishes to be picked up and starts the trip. A driver reports her route and departure time to the platform before seeing a list of passengers.

Passenger List The driver sees a sorted list of passengers based on her route and departure time. The sorting algorithm's key input is a **compatibility score** that measures route similarity. The score is calculated as the distance of the passenger trip divided by the total distance of the trip, which is the distance from the driver origin to the passenger pickup location, then to the passenger destination and finally to the driver's own destination. The algorithm also sorts passengers based on the similarity of departure times. A driver can view all requests via the platform's app, and the first driver who answers a request is matched with the corresponding passenger.

Driver Interface The left panel of Figure 1 is the driver view. A driver first inputs her trip information (origin and destination of the trip; a departure time indicating the time when she wishes to start driving). She can then see a list of passengers sorted by the compatibility score (displayed alongside the passenger's departure time), distances between driver and passenger origins, distances between their destinations and the trip fare. Passengers with similar departure times are also ranked higher. The fare is strictly based on the passenger trip distance with a slight discount on longer trips.[5] A driver can check the list of waiting passengers at any time.

[5]The observed fare can be well approximated by a 6th order polynomial of trip distances. The resulting fit has a mean squared error of \$0.003. In comparison, the mean and standard deviations of the fares are \$4.84 and \$2.5. All units are in 2018 USD.

Figure 1: Driver and Passenger Interfaces

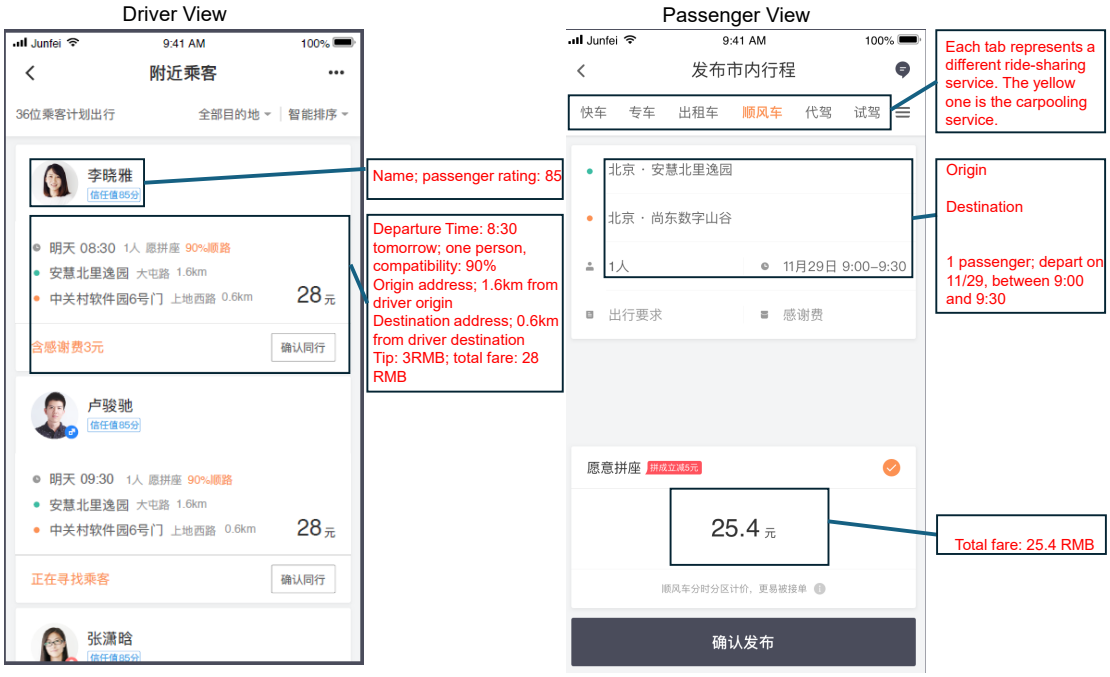

Passenger Interface The right panel of Figure 1 is the passenger view. The top tab shows 6 different platforms by the same company. The first one is the company's main ride-hailing platform that uses a centralized algorithm to assign a driver to a passenger request. Similar to Uber or Lyft, most drivers on the platform are full-time. This platform is also the largest, completing 41 million trips per day in 2023. The yellow tab is the carpooling platform we study. The passenger using the carpooling platform needs to fill out the trip origin, destination and departure time. She can additionally indicate the number of people per ride, a range for the departure time as opposed to a time point, whether she is willing to share a ride with another passenger, and whether to include a tip. In our data, we find ride-sharing with other passengers and tipping to be rare (<4% of all requests), and all passengers input time points for the departure time. Our empirical analysis thus focuses on one-driver-to-one-passenger-request matching, where fares are distance based and departure times are time points.

Pickup and Dropoff Passenger pickup and dropoff occur after a driver confirms a match with a passenger. The driver will travel to the passenger's origin and pick up the passenger by the departure time set by the passenger. The driver then follows a route set by the app to deliver the passenger to the passenger's destination. The passenger is charged the fare after the dropoff. The platform receives 10% of the fare and the driver receives the rest.

Table 1: Summary Statistics

	Mean	Quantile		
		25%	50%	75%
(a) Driver				
Characteristics				
Distance (km)	24.30	13.49	20.30	30.02
Arrival to Departure Time (Minutes)	18.02	5.10	17.33	29.37
% Start in Downtown	26.59			
% End in Downtown	24.63			
Search				
% Wait After Arrival	39.97			
Duration (Minutes) | Wait After Arrival	17.20	8.10	14.56	24.43
Number of Searches | Wait After Arrival	3.65	2	3	4
Number of Driver Trips		32,621		
(b) Passenger				
Characteristics				
Distance (km)	21.16	11.19	18.17	28.11
Fares ($)*	4.84	3.01	4.43	6.18
Arrival to Departure Time (Minutes)	20.10	14.63	17.48	29.30
% Start in Downtown	31.21			
% End in Downtown	27.43			
Search				
% Wait After Arrival	84.14			
Duration (Minutes) | Wait After Arrival	6.38	1.12	3.43	8.83
Duration (Minutes) | Matched	5.04	0.88	2.30	6.40
% Matched	44.24			
% Matched | Wait After Arrival	52.58			
# of Matches Per Day | Arrival Time 4:30 pm-5:00 pm**	421.70			
Revenue ($)* Per Day | Arrival Time 4:30 pm-5:00 pm**	2172.42			
Number of Passenger Requests		19,064		

Arrival times for drivers are defined as the first time they search for passengers. Arrival times for passengers are defined as the time they send a request. For those that did not send a request, the arrival time is the time they opened the main ride-hailing tab on the interface. For drivers, "Wait after arrival" means that a driver searches for passengers for at least two times. For passengers, "Wait after arrival" means that the passenger sends a request on the carpooling platform.

*: Fares are in 2018 USD.

**: Averaged across 20 days in the sample

3.2 Data

Samples

Our data cover an afternoon period of 20 weekdays in 4 consecutive weeks in May and June of 2018 in one city of 8.8 million population. We observe all drivers with trip departure times between 5:00 pm and 5:20 pm. The dataset contains the reported driver routes (origin and destination coordinates), departure times and the time stamps when a driver checks the waiting passengers, which we refer to as a search. We observe all search instances of each driver.

We also observe all passengers sending ride requests between 4:30 pm and 5:00 pm (regardless of trip departure times). Information of each request includes coordinates of the route, the time the request is sent, and the departure time of each request. We also observe the match outcomes. If a passenger is matched, we observe the time of the match and the ID of the matched driver. The data reflect matching for late-afternoon intracity commuting on the platform. A survey of Chinese carpooling platform passengers shows that morning and afternoon commuting needs account for 64% of the rides (China Daily, 2023).

Summary Statistics

Panel (a) of Table 1 summarizes the driver search data. We define a driver trip as a driver-day combination. We observe 32,621 trips and 17,966 unique drivers. The summary statistics are based on driver trips, because repeat drivers may have different routes or departure times across days. The first part of the table looks at trip characteristics. On average, the trip length is over 20 km, which is about four to five times of the average taxi trips in China (Liu, Gong, Gong and Liu, 2015) or the US (Buchholz, 2022). Drivers arrive about 18 minutes before the departure time. For locations, we find that although the downtown area accounts for less than 5% of the land area of the city, it contains around 25% of drivers' trip origins or destinations. The second part of the table provides statistics on driver search behaviors. We find that a majority of drivers (60%) do not search again after arrival and leave the market. These drivers that left after one search might have made a match or decided to leave without a match. For drivers that do wait in the market after arrival, we define a driver's search duration as the time difference between her first and last search. The average duration is 17 minutes, and a driver searches two to four times. The last search on most of the driver trips are before or very close to the departure times. About 21% of the last searches are after the departure. Within these trips, 74% exceed the departure by less than 1 minute, and 99.86% exceed the departure time by less than 5 minutes.

Due to the different time windows of the driver and passenger samples, we observe only a subset of driver trips' match outcomes. Specifically, we are able to link 12% of the driver trips to passenger requests in our sample. For the rest of the trips, a driver might have matched with a passenger that arrived outside the 4:30 pm-5:00 pm time window, or left the market without a match.

On the passenger side, we can link 47% of the matched passenger-driver pairs to drivers in our driver data. We also note that a passenger may be matched with a driver not in our sample (i.e. a driver with a departure time outside the 5:00 pm to 5:20 pm window). If a request is canceled (the

passenger leaves the market without a match), we observe the time of the cancellation. To mirror the drivers who search only once, we additionally construct a set of potential passengers that arrive to the app but do not use the carpooling service based on the browsing data of the main ride-hailing platform.[6] Panel (b) of Table 1 summarizes the passenger data. We observe a total of 19,064 requests across 20 days by 14,162 passengers. Like the driver side, all statistics are based on requests. We find that the passenger and driver trip lengths are similar, with an average fare of $4.84. Passengers arrive about 20 minutes before their departure times. Over 80% of passengers decide to wait after arrival. The average search duration of the passengers that decide to wait, defined as the time difference between arrival and the time of the match or cancellation, is 6.38 minutes, substantially shorter than drivers'. Most of the passenger requests are answered or canceled before the departure times (99.76%). On average, 974 passengers arrive at the platform per day and 422 of them are matched during our data window.

3.3 Descriptive Results

Matching Across Days

We begin our analysis by examining the carpooling platform as a two-sided market, where more drivers entering the market relative to passengers intuitively increases the percentage of matched passengers. Figure 2 illustrates this relationship by plotting the daily driver-to-passenger ratio against the percentage of matched passengers. The ratio is defined as the number of drivers divided by the number of passengers for each day in our dataset.[7]

Determinants of Matches

We next identify a set of characteristics critical for the driver decisions. Specifically, we construct a dyadic dataset where each instance of a driver searching for passengers is linked to the set of passengers available at that time.[8] Each dyad consists of a driver who searches at a time t and a passenger waiting at t. A waiting passenger is defined as one whose arrival time is before t and whose match or cancellation time is no earlier than t. Despite observing only a subset of waiting passengers (those arriving between 4:30 pm and 5:00 pm), we find robust patterns that matched driver-passenger pairs are significantly more compatible than the unmatched.

Table 2 shows that the average compatibility score[9] is 0.47 for all dyads, compared with 0.83 of dyads that correspond with a match. The matched dyads are also more compatible on other dimensions

[6] The main ride-hailing platform is similar to Uber or Lyft, and it is accessible as the first tab of "other ride sharing services" on the passenger view of the interface in Figure 1. For each of the 20 days in our sample, we define potential passengers on a day as those that (1) entered trip information on the passenger interface of the main ride-hailing service of the platform between 4:30 pm and 5:00 pm, (2) did not send a carpooling request on this day, and (3) sent at least one request on our carpooling platform on a different day. The search duration of these potential passengers are set to 0.

[7] This ratio serves as a proxy for the relative number of arriving drivers per passenger under the assumption of uniform arrival rates over time. Although we cannot directly test whether drivers arrive at a uniform rate, we find that passengers do (Online Appendix SA.1).

[8] We construct the dyads based on a maximum of 85 passengers sorted by the compatibility scores for each driver search instance. The statistics in this section change minimally if we include more passengers.

[9] We do not directly observe the score from data and instead use the formula described in Section 3.1 to compute the score.

Figure 2: Share of Matched Passengers Across Days

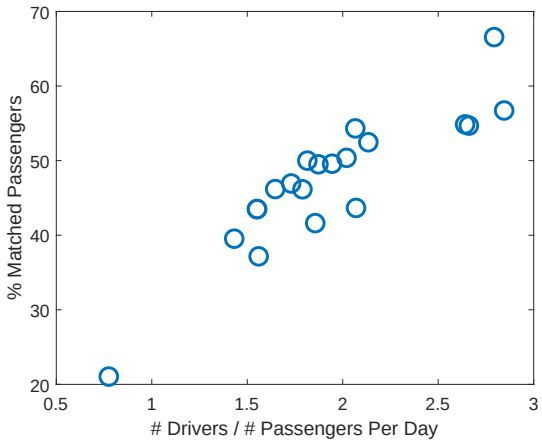

Note: The x axis is the number of drivers divided by the number of passengers in our dataset. The y axis is the share of matched passengers. The x variable is proportional to the ratio of the number of entering drivers to the number of passengers in a unit time.

such as the distances between origins (pickup distances) and destinations (dropoff distances) and departure time differences. The fares of matched dyads are also higher.

Leaving Probability and Departure Time

Next, we show that drivers are more likely to leave or match closer to departure, consistent with forward-looking behaviors and falling waiting values. We demonstrate this result in Figure 3. In panel (a), the red line shows the average probability of a driver leaving[10] between $\tilde{t}$ and $\tilde{t}-5$ minutes before the departure time, conditional on the driver waiting at $\tilde{t}$ minutes before departure. The plot shows that this probability is higher when drivers are closer to departure.

We next rule out that this increase is due to a driver heterogeneity, where drivers who arrive closer to departure may be more impatient. We estimate the marginal effects of waiting time since arrival on the leaving probability. For each $\tilde{t} = 45, 40, \ldots, 5$, we define $y_{i\tilde{t}} = 1$ if a driver i is in the market $\tilde{t}$ minutes before the departure time but matches with a passenger or leaves in the next 5 minutes, and $y_{i\tilde{t}} = 0$ otherwise. For each subsample of drivers who are in the market $\tilde{t}$ minutes before the departure time, we regress $y_{i\tilde{t}}$ on driver i's waiting time since arrival.[11] The blue line in Figure 3(a) represents the estimated marginal effect of having waited an additional 5 minutes. The marginal effect is nearly 0 with a tight 95% confidence interval for drivers whose arrival time is within 40 minutes of departure time, which account for more than 91% of all drivers. The results suggest that, given the same time

[10] Given our data restriction, we are able to match drivers to only a subset of passengers. Therefore we do not distinguish whether a driver matches with a passenger or leaves unmatched here. In Online Appendix SA.2, based on the driver data linked to passengers, we estimate the effects of driver-passenger compatibility measures and driver's time to departure on the probability of matching with a passenger in our data in a dyadic regression. We find that drivers closer to departure time are more likely to form matches.

[11] We also control for whether the trip distance is between 10 and 30 km, whether the trip length is greater than 30 km, whether the trip starts in downtown and whether the trip ends in downtown.

Table 2: Driver-Passenger Dyadic Statistics

	Mean	Quantiles		
		25%	50%	75%
All Dyads				
Compatibility Score	0.47	0.30	0.43	0.60
Pickup Distance (km)	15.09	8.84	14.94	21.44
Dropoff Distance (km)	15.63	9.34	15.80	22.07
Fare ($)	4.42	2.93	3.98	5.41
Departure Time Difference (Minutes)	-2.88	-13	0	10
Number of Dyads		2,449,963		
Matched Dyads				
Compatibility Score	0.83	0.76	0.85	0.93
Pickup Distance (km)	2.73	0.99	1.97	3.48
Dropoff Distance (km)	3.79	1.10	2.35	4.69
Fare ($)	5.55	3.84	5.10	6.62
Departure Time Difference (Minutes)	0.63	-6	0	10
Number of Dyads		3,970		

Note: pickup and dropoff distances are distances between origins and between destinations. Departure time difference is defined as the driver departure time minus the passenger departure time in a dyad. Fares in 2018 USD.

remaining until departure, drivers arriving closer to their departure time are not more likely to leave.

We repeat this exercise for passengers. In panel (b), we compare the mean passenger probability of leaving with the estimated effects of waiting time since arrival. We find that the effects of waiting time are low even for passengers that arrive more than 40 minutes from the departure time.

Drivers Are Less Selective Closer to Departure

Finally, we show that drivers accept less compatible passengers closer to departure. This pattern is also consistent with decreasing values of waiting. In Figure 4, we plot the the matching time against the compatibility scores, pickup distances and dropoff distances of matches separately. We find that, closer to departure, the compatibility scores slightly fall and the dropoff distances are unchanged, but the pickup distance just before departure is statistically significantly higher than the distances in earlier matches.

3.4 Interviews

We conducted interviews with drivers to further understand two key questions about driver choices: (1) how do drivers evaluate match quality? (2) How do they evaluate the values of waiting? We hired 9 college student to interview 34 drivers in two waves in July 2021 (12 drivers) and in October and November 2022 (22 drivers). Online Appendix SB describes the details of interviews.

The interviews with drivers confirm our descriptive results. Drivers state that the most important factors of match quality are the similarities of routes and departure times. Drivers also reveal that

Figure 3: Leaving Probability and Waiting Time

(a) Driver

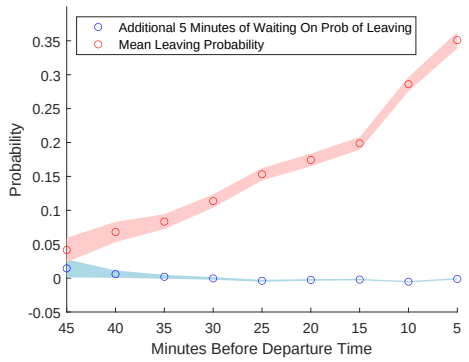

(b) Passenger

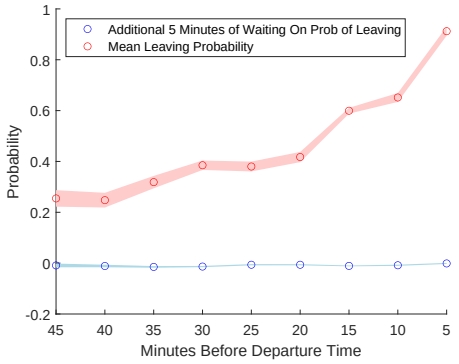

Note: the color fill indicates the 95% confidence intervals based on robust standard errors.

Figure 4: Match Quality Over Time

(a) Compatibility Score

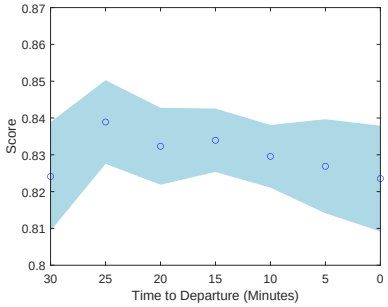

(b) Pickup Distance (km)

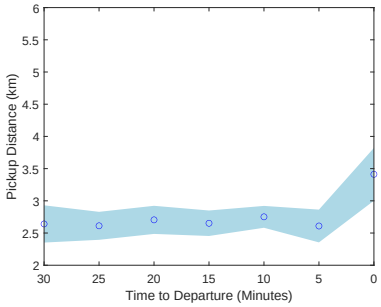

(c) Dropoff Distance (km)

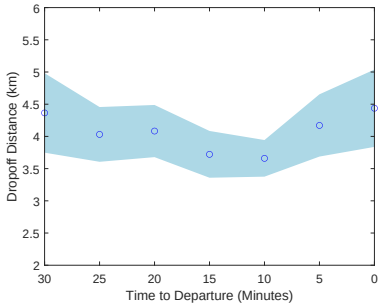

Note: each circle at t represents the average score or distance of the matches within $t-5$ to t minutes from the driver's departure time. The color fill indicates the 95% confidence intervals.

they are less likely to wait and less sensitive to the match quality near the departure time.

We also interviewed the hired students to understand how passengers make the decision to wait or leave. A key input to this decision is the passenger's belief about when the request is likely to be answered. A survey of our interviewers shows that they can identify a time window during which matches occur. We asked interviewers to recall when and how likely they were matched. We explicitly instructed them to report their subjective beliefs without checking their order history. We find that the match time depends on the departure time (regardless of when the requests were sent). The time windows of matching range from within 20 minutes to within one hour before the departure time, depending on the origins and destinations of the trips. Our interviewers did not perceive the match rate to be different within the time window.

4 Empirical Model

We consider a continuous-time dynamic matching model between drivers and passengers with a discrete set of routes and trip departure times. Each unique combination of a route and departure time defines a **type**. There are K types of drivers and L types of passengers.

4.1 Drivers

Type k drivers arrive exogenously to the market before their departure time T_k and decide to match, wait or leave. If a driver decides to wait, she moves again at rate $\lambda_k(t)$ and chooses from the three actions. In our setting, moves that occur at random times represent instances of a driver checking the passengers on the phone. We allow the move arrival rate $\lambda_k(t)$ to depend on both the driver type and the clock time t. The rate can thus, for example, be higher when t is close to the departure time T_k.

Primitives

We focus on a driver i of type k. When the driver moves at t, her actions are associated with independent, driver specific extreme value type 1 (EV1) shocks $\varepsilon_{it} = \left(\varepsilon_{it}^{\text{match}}, \varepsilon_{it}^{\text{leave}}, \varepsilon_{it}^{\text{wait}}\right)$. We assume that driver i's value for matching with a passenger j of type ℓ is $u_{ijt} = u_{ij} + \varepsilon_{it}^{\text{match}}$, where $u_{ij} = u_{k\ell} + \sigma\nu_{ij}$. The term $u_{k\ell}$ represents the compatibility of routes and departure times between types, and ν_{ij} is an i.i.d. idiosyncratic driver preference shock for a passenger with the standard normal density ϕ. The parameter σ captures the size of the shock. The value of leaving the market without a match is $u_{k0} + \varepsilon_{it}^{\text{leave}}$. The driver also incurs a flow waiting cost $c_k(t)$.[12]

Beliefs

We use $p_k(t)$ to denote the probability that the observed set of passengers $\mathfrak{S}_t$ is non-empty at t. The driver also forms a belief about the highest passenger value net of the EV1 shock $u = \max_{j \in \mathfrak{S}_t} u_{ij}$. We use $G_k(u;t)$ to denote, conditional on $\mathfrak{S}_t \neq \emptyset$, the distribution of u at time t. An important

[12] This specification allows us to specify waiting cost dependent on the departure but not arrival time. This restriction is reasonable in our setting, because our descriptive results show that the driver decisions to leave depend primarily on time to departure.

simplifying assumption is that drivers do not use past choice sets in her inference of u. This assumption is consistent with our interviews with drivers (Online Appendix SB.2).

Value Function

A driver chooses between matching, waiting and leaving. After integrating over the driver-specific EV1 shocks ε_{it}, we can show that the expected waiting value V_k for a type k driver is given by the following Bellman-Hamilton-Jacobi equation:

$$\begin{aligned} 0 = \lambda_k(t) \cdot \Bigg(\Upsilon + p_k(t) \int \ln\left(\exp(u) + \exp\left(V_k(t)\right) + \exp\left(u_{k0}\right)\right) dG_k(u;t) \\ + \left(1 - p_k(t)\right) \ln\left(\exp\left(V_k(t)\right) + \exp\left(u_{k0}\right)\right) \Bigg) + \frac{dV_k}{dt} - \lambda_k(t) V_k(t) - c_k(t), \end{aligned} \tag{1}$$

with the boundary condition $V_k(T_k) = u_{k0}$. We assume that any type k driver who does not match or leave before T_k will leave at T_k. We can normalize u_{k0} to 0 by subtracting it from both the match value and the waiting value.[13] We provide the expressions for normalized driver choice probabilities in Appendix A.1.

4.2 Passengers

Similarly, type ℓ passengers arrive exogenously before the departure time T_ℓ. We use v_j to denote a passenger j's value for being matched and v_{0j} for the value of the outside option.[14] We assume that, for a type ℓ passenger j, $v_j - v_{0j} = v_\ell + \xi_j$, where ξ_j is i.i.d. and follows the logistic distribution. The passenger incurs an increasing waiting cost $o_\ell(t)$ at t, which increases in t. Consistent with our student interviews, we keep the passenger belief simple and assume that a type ℓ passengers form belief about the average match rate γ_ℓ. The belief remains constant over time but differs across types.

At a time t, the passenger j chooses an optimal leaving time $t_j^\star$ to maximize the expected value of waiting:

$$W_j(t) = \max\left\{ v_{0j}, \max_{t_j^\star \leq T_\ell} \int_t^{t_j^\star} \gamma_\ell \left(v_j - o_\ell(\tau)\right) \exp\left(-\gamma_\ell(\tau - t)\right) d\tau \right\}. \tag{2}$$

With a constant γ_ℓ, the optimal solution $t_j^\star$ does not depend on t. The solution implies the following passenger decision rules: an arriving passenger leaves immediately without sending a request if $t_j^\star$ is earlier than the arrival time; if a passenger is not matched by $t_j^\star$, she cancels her request and leaves unmatched.

[13] In a more flexible model, the outside option value may also vary over time. A similar normalization shows that we can set both c_k and u_{k0} to 0 and specify a time-varying match value function u. In practice, we have found it challenging to separately estimate the value function and time-varying match values with our data.

[14] As on the driver side, we similarly restrict the outside option of the passenger to be time-invariant. In principle, we can allow the outside option and thus the normalized match value v_ℓ to be time-varying. The variation of beliefs across types can potentially separately identify the time-varying components in the match value from those in the cost function. In practice, we have found it hard to separately estimate the two sets of primitives. We thus fix the outside value to remain constant over time and focus on identifying the waiting cost.

After integrating over ξ_j, the probability of a type ℓ passenger setting the optimal leaving time after t is

$$S_\ell\left(t;\gamma_\ell\right) \equiv \Pr\left(t_j^\star > t\right) = \frac{1}{1+\exp\left(o_\ell\left(t\right)/\gamma_\ell - v_\ell\right)}. \tag{3}$$

Differentiating S_ℓ with respect to t yields the rate at which type ℓ passengers leave without a match.

4.3 Equilibrium

We relegate the details to Appendix A. Our matching equilibrium consists of a set of conditions that endogenize the driver beliefs about the distribution of passengers, passenger beliefs about the match rates, the values of waiting, the driver choice probabilities, the passenger leaving rates and the transitions of the masses. A key simplifying feature of the model is that an individual driver or passenger is atomless, and each type has a unit mass. In the equilibrium, each type's mass continuously change over time as agents arrive, match and leave. Agent beliefs at any time need to be consistent with the corresponding equilibrium masses. We interpret the equilibrium outcome as an approximation of a matching market with a large number of discrete and heterogeneous agents. The agent masses and matched masses are fractional analogs of the number of agents and number of matches. Ostrovsky and Schwarz (2018) calls the resulting matches "quasi-assignments".

5 Driver Estimation

The structural parameters on the driver side are match preferences $u_{k\ell}$ and waiting costs $c_k\left(t\right)$. Our identification and estimation proceed in two steps. The first step directly identifies the match utility $u_{k\ell}$, the size of σ and the value function. The second step inverts the waiting costs $c_k\left(t\right)$ from the value functions.

5.1 First Step

Given a set of passengers $\mathfrak{S}_t$ when a driver moves at the clock time t, the driver model in Section 4 shows that the probability of a driver i choosing a passenger j is

$$p_{ij}\left(t\right) = \int \underbrace{\prod_{\substack{j' \neq j \\ j' \in \mathfrak{S}_t}} \Phi\left(\frac{u_{k(i)\ell(j)} - u_{k(i)\ell(j')}}{\sigma} + \nu_{ij}\right)}_{\Pr(j \text{ is the best match})} \underbrace{\frac{\exp\left(u_{k(i)\ell(j)} + \sigma\nu_{ij}\right)}{1+\exp\left(u_{k(i)\ell(j)} + \sigma\nu_{ij}\right) + \exp\left(V_{k(i)}\left(t\right)\right)}}_{\Pr(\text{matching with } j \text{ given it is the best match})} \phi\left(\nu_{ij}\right) d\nu_{ij}, \tag{4}$$

where $k\left(i\right)$ and $\ell\left(j\right)$ denote i's and j's types. We can similarly write down the probability of leaving. These probabilities form the basis of our identification and estimation.

We specify the match utility as

$$u_{k\ell} = \beta_z z_{k\ell} + \beta_x x_k + \beta_f f_\ell + \beta_k. \tag{5}$$

In the above, $z_{k\ell}$ is a vector of variables that measure the compatibility between the driver and passenger types,[15] which includes the compatibility score used by the platform, the pickup and dropoff distances, whether departure time differences are less than 5 minutes, whether the differences are less than 15 minutes, and whether the passenger has a later departure time than the driver. The vector of variables x_k includes the type k's route distance, whether the trip starts in downtown, and whether the trip ends in downtown. We use f_ℓ for a type ℓ passenger's fare. The parameter β_k captures the unobserved heterogeneity in match preference, which is the same for drivers of the same type but could differ across types. We assume β_k has a discrete distribution.

We next flexibly specify a driver's value function. We parameterize the value function as $V_k(t) = \mathrm{V}(T_k - t, x_k, \Theta_k)$, where Θ_k is a vector of type-specific random coefficients. We provide the specification in Online Appendix SC. Importantly, our specification accommodates observed and unobserved heterogeneity through type-specific covariates x_k and a vector of random coefficients Θ_k. A simplifying restriction is that the value function depends on time to departure but not time waited, which is consistent with driver behavior documented in Section 3.3. We jointly identify and estimate the distribution of unobserved heterogeneity in both the match utility and value function (β_k, Θ_k).

5.1.1 Identification

We assume that the arrival times of drivers are independent of unobservables, and her move arrival rates only depend on observed characteristics (routes and departure times).

Assumption 1. *Identification of Driver Parameters*

1. *Driver arrival times are independent of unobserved shocks* $(\nu_{ij}, \varepsilon_{it})$ *and unobserved heterogeneity* (β_k, Θ_k).
2. $\lambda_k(t) = \lambda(t; route_k, T_k)$.

The assumptions rule out that the timing of driver actions is correlated with unobservables, and we can thus use the variations in driver characteristics, choice sets, and arrival timing to identify the driver choice model.

Match Preference Parameters $\beta_z, \beta_f, \beta_x$ The variation of passenger characteristics in the choice set $\mathfrak{S}_t$ identifies β_z. For example, if z is the compatibility score, we can compare the match decisions of drivers when they face passengers that have different compatibility scores but are otherwise observably identical. The differences in the match probabilities identify β_z. Similar arguments apply to other match specific regressors. The formal identification argument builds on the idea of special regressors (Manski, 1988; Lewbel, 2014, 2019).

Identifying β_x in the match preference relies on the variations of driver characteristics (such as whether the starting point is in a key region or trip distance), which change the values for matching with a

[15] In estimation, we treat the characteristics of each observed driver as representing a driver type. Therefore $x_{k(i)}$ corresponds with the trip characteristics of driver i. We also treat the characteristics of each observed passenger as representing a passenger type, and $z_{k(i)\ell(j)}$ measures the compatibility of trip characteristics between i and j.

passenger across drivers. For example, a high β_x on long-distance drivers corresponds with these drivers making more matches, holding other covariates equal.

Match Specific Unobservables σ The variation in the size of $\mathfrak{S}_t$ identifies σ. Intuitively, $\sigma > 0$ indicates that a driver's match probability increases if we duplicate her choice set of potential passengers,[16] and the level of increase identifies the magnitude of σ. This intuition is similar to the identification of multinomial choice demand models based on variations in consumer choice sets (Berry and Haile, 2014).

Value Function V Variations in arrival times relative to departure times identify the driver value of waiting as a function of $T_k - t$. For example, we can compare the decisions of two drivers who have the same route and arrive at t, where one driver's departure time is $t + 20$ and the other's is $t + 30$. If the value function decreases sharply around $T_k - t = 20$, the driver closer to the departure time is more likely to choose a passenger or leave immediately than the other driver. The key assumption here is that the arrival time is independent of driver preferences for matches or waiting costs. A different assumption that also rationalizes the data is that drivers arriving earlier relative to their departure times have lower waiting costs. In this case, we would expect the probability of leaving to be negatively correlated with the amount of time the agent has waited in the market. Section 3.3 shows this correlation to be small for most drivers and passengers. Furthermore, we consider a robustness analysis where we include the arrival-to-departure times as covariates in the value function. Online Appendix SA.7 shows that the estimated waiting costs are very similar.

Unobserved Driver Heterogeneity To identify the unobserved heterogeneity, we group drivers by their origins and destinations and use the panel structure of the data. Specifically, we divide the city into 2 km-by-2 km square regions. We assume that (β_k, Θ_k) are the same for the drivers whose origins and destinations are in the same pair of 2 km-by-2 km square regions, and the heterogeneity is distributed independently across these regions. The heterogeneity captures the similarity of driver preferences based on workplace or home similarity. For example, drivers leaving from downtown to a residential area with expensive housing are likely to have higher incomes and weaker preferences for matches. We assume that the heterogeneity has a discrete distribution. The formal identification argument follows from the literature on the finite-mixture dynamic discrete choice models with panel data (Kasahara and Shimotsu, 2009). For intuition, consider the case where we observe many drivers for each pair of regions. Within a region $\mathfrak{r}$, the variations of choice sets and driver arrival times identify

[16] Specifically, we compare two drivers with the same characteristics but facing different choice sets. A larger σ corresponds with a higher probability that a driver matches with any passenger when $\mathfrak{S}_t$ is larger. Suppose one driver's choice set has 1 passenger. We use $q(1;\sigma)$ to denote the probability that driver finds a match. The other driver's choice set has 2 passengers with routes and departure times similar to the first driver's. We use $q(2;\sigma)$ to denote this driver's match probability. The match probabilities depends on driver preferences for passenger characteristics and the shocks ν_{ij}. We argue that σ increases the difference of the match probabilities $q(2;\sigma) - q(1;\sigma)$. In the extreme case where $\sigma = 0$, the match probability difference should be close to 0. In the case where σ is extremely large, a match occurs whenever the normally distributed ν_{ij} is positive. If, for example, the match value and waiting value are both 0 and σ is large, the probability of a match would be 50% with a single passenger (50% probability that ν_{ij} is positive), but 75% with two passengers. Therefore the choice probability difference $q(2;\sigma) - q(1;\sigma)$ would be 25% in this case.

the heterogeneity $(\beta_{\mathfrak{r}}, \Theta_{\mathfrak{r}})$. Then the distribution of $(\beta_{\mathfrak{r}}, \Theta_{\mathfrak{r}})$ across regions identifies the distribution of the heterogeneity.

Discussion: Direct Estimation of Structural Parameters in $u_{k\ell}$ Notably, the estimation of structural parameters in the driver preference function does not require directly solving the driver decision problem, unlike other conditional choice estimators of dynamic models (e.g., Hotz and Miller 1993; Bajari et al. 2007). The reason is that drivers do not form expectations about future matches based on the current choice set.[17] Therefore the choice set variations identify the match preference parameters separately from the value of waiting. However, we emphasize that the value function parameters are not structural parameters. We use the estimated value functions and the dynamic driver decisions to invert the structural waiting costs in the next section. When we simulate the counterfactual market equilibrium, the value functions are re-computed under alternative matching policies.

5.1.2 Estimation

The estimation based on Eq. (4) would be straightforward if we observe the full set of $\mathfrak{S}_t$. However, we observe only passengers that arrive between 4:30 pm and 5:00 pm and are still unmatched and active at time t, which are a subset of $\mathfrak{S}_t$. We discuss how we simulate the "missing" passengers in Online Appendix SA.4. The procedure first computes the mass transitions of passengers arriving outside the data time window and then simulates whether a passenger is in a driver's choice set.

We account for these missing passengers, preference shocks ν_{ij} and unobserved heterogeneity in a simulated maximum likelihood estimator.[18] Our baseline estimates are based on a 2-component finite mixture model. We also report estimates with 3 unobserved components.

Estimation Results Table 3 reports the estimated match preference parameters in (5). We find that drivers have strong preferences for route compatibility. The willingness to pay for ten percentage points increase in compatibility scores is $(10\% \times 2.97/0.10 =)2.97$ dollars, which are about half of the average fares in the data. Other estimates are also reasonable: drivers dislike longer pickup or dropoff distances or large differences between departure times. We also find that drivers starting or ending in downtown areas have weaker preferences for matches. In addition, there is substantial match level heterogeneity, where the standard deviation σ of match specific preferences ν is valued over \$8. Finally, we find some evidence of driver heterogeneity, where the difference of match values between the two types of β_k is about \$3.

The estimated value function contains a large number of parameters, and we report the estimates in Online Appendix SA.5. The estimates are consistent with our descriptive results. We find, for

[17] Our model differs from models of oligopolistic dynamic games (e.g. Ericson and Pakes 1995), where an agent tracks the states of all other agents.

[18] The likelihood for each driver search instance corresponds with the probability of matching, waiting or leaving given the actual choice observed in the data, where a driver's choice set is a combination of actual passengers in the data and the simulated passengers. The likelihood function first integrates the choice probabilities in (4) for each moment a driver searches over simulated sets of passengers and unobserved preferences ν_{ij}. The function then integrates over the joint likelihood of drivers traveling to and from the same pairs of 2 km-by-2 km squares over the distribution of (β_k, Θ_k).

Table 3: Driver Preferences for Matches

	2-Component	3-Component		2-Component	3-Component
Match Specific Characteristics β_z			Fares β_f	0.10	0.10
				(0.01)	(0.01)
Compatibility Score	2.97	3.21			
	(0.13)	(0.15)			
Pickup Distance	-0.29	-0.30	Unobserved Preference		
	(0.01)	(0.01)	For Passengers σ	0.86	0.92
Dropoff Distance	-0.19	-0.20		(0.02)	(0.03)
	(0.00)	(0.01)			
Dptr. Time Difference	0.05	0.04			
≤ 5 Minutes	(0.03)	(0.03)	Unobserved Match Preference		
Dptr. Time Difference	0.30	0.28	Component 1		
≤ 15 Minutes	(0.03)	(0.04)	β_k	-2.89	-3.95
				(0.14)	(0.24)
Passenger Dptr. Time	-0.49	-0.53	Prob	0.53	0.28
Later Than Driver's	(0.03)	(0.03)		(0.02)	(0.03)
Driver Specific Characteristics β_x			Component 2		
			β_k	-2.56	-2.83
Distance 10-30 km	0.19	0.22		(0.14)	(0.16)
	(0.08)	(0.09)	Prob	0.47	0.44
Distance>30 km	-0.00	0.03		(0.02)	(0.02)
	(0.11)	(0.12)	Component 3		
Start in Downtown	-0.41	-0.43	β_k		-2.15
	(0.05)	(0.05)			(0.19)
End in Dowtown	-0.15	-0.14	Prob		0.28
	(0.05)	(0.05)			(0.04)

Note: we report standard errors in parentheses.

example, that waiting values are lower near departure. We also find that drivers to or from downtown have higher values of waiting. The next section describes how to recover waiting costs based on these estimates.

5.2 Second Step

Given the driver value function in (1), the waiting cost can be inverted as

$$c_k(t) = \lambda_{kt} \cdot \Big(\Upsilon + p_k(t) \int \ln\left(\exp(u) + \exp\left(V_k(t)\right) + 1\right) dG_k(u;t) \\ + \left(1 - p_k(t)\right) \ln\left(\exp\left(V_k(t)\right) + 1\right) \Big) + \frac{dV_k}{dt} - \lambda_{kt} V_k(t). \tag{6}$$

Identification

The above identifies the waiting cost because the right hand side consists entirely of known quantities. To see this, we note that the first step in Section 5.1 identifies $u_{k\ell}$ and V_{kt}. We can then use the estimated driver-passenger match values $u_{k\ell}$ and the equilibrium beliefs defined in Appendix A to compute the probabilities that the driver choice is non-empty, $p_k(t)$, and the distribution of the highest match value $G_k(u;t)$.

The identification of the waiting cost is related to the literature on identifying discount factors in dynamic models (e.g., Rust 1994; Magnac and Thesmar 2002; Abbring and Daljord 2020). The

Figure 5: Waiting Cost Estimates

(a) Driver

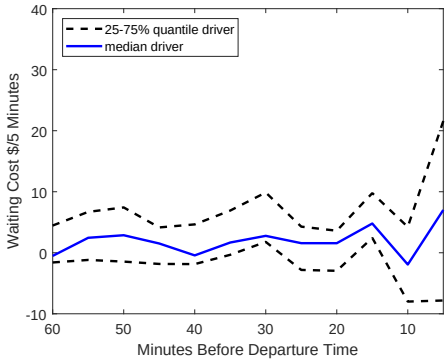

(b) Passenger

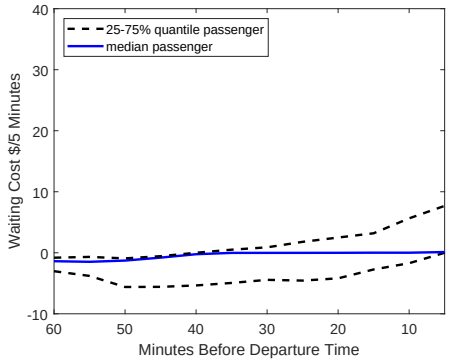

Note: The waiting costs are in units of $/5 minute in 2018 USD. For a given 5-minute interval, points on the black broken lines represent the 25% and 75% quantiles of waiting costs across drivers or passengers. The blue line represents the median costs. The waiting costs could reflect the cost of time and the income of the users, where the high level of heterogeneity is consistent with the large income inequality in China documented in Piketty et al. (2019). An interpretation of a negative driver waiting cost is that a driver has not finalized her trip (such as whether to share rides on the platform or offer a ride to a colleague) and prefers delaying a match. A negative passenger waiting cost could reflect saved opportunity costs of planning alternative transports (such as delaying the need to look up bus schedules).

typical approach of identification relies on instruments that vary the expected future values but not the instantaneous payoffs. In our setting, the exogenous arrival time is such a variable. As we discussed in the previous section, the variation in arrival time identifies the value function, which in turn allows us to identify waiting costs through Eq. (6).

Estimates

The inversion of waiting costs can be done for every driver type and for each component of unobserved heterogeneity. We visualize the waiting cost distribution in panel (a) of Figure 5. Specifically, we compute the distribution of the waiting costs across drivers for every 5-minute interval within one hour from the departure time, and we plot the median and the 25%-75% quantiles of the waiting costs. The median waiting costs are low and remains at about 0 until the last 15 minutes before departure. The waiting costs could reflect the cost of time, which is likely correlated with the income of the drivers. The high level of heterogeneity is consistent with the large income inequality in China documented in Piketty, Yang and Zucman (2019). An interpretation of a negative waiting cost is that a driver has not finalized her trip (such as whether to share rides on the platform or offer a ride to a colleague) and prefers delaying a match.

5.3 Other Components of the Driver Model

In addition to preferences for matches and waiting costs, the number of types, routes, arrival times, departure times and arrival rates of moves are also inputs to the simulation of the full equilibrium model in Section 4.

Types In the simulation procedure described in Online Appendix SD.1, we explain how we construct types. We assume that the arrival times approximate a Poisson process, and we find that an aggregate arrival rate of 77.6 drivers/minute allows us to match the number of drivers with departure times between 5:00 pm and 5:20 pm (1631 drivers per day) with our data. We simulate the arrival times of drivers based on this Poisson distribution. We then simulate each driver's routes and departure times according to their empirical distributions.

Arrivals of Moves Consistent with Assumption 1, we estimate the move arrival rate, which corresponds with the frequencies of drivers checking the list of passengers on their phones. The estimates show that drivers search more frequently closer to the departure time. The details can be found in Online Appendix SA.6.

6 Passenger Estimation

We estimate the passenger utility v_ℓ and waiting cost $o_\ell(t)$. We assume $v_\ell = \zeta_x x_\ell - \zeta_f f_\ell + \zeta_\ell$, where x_ℓ consists of whether a passenger's trip starts in downtown and whether it ends in downtown, f_ℓ is the fare and ζ_ℓ captures the passenger unobserved heterogeneity. We specify a flexible passenger cost function $o_\ell(t)$ that has a similar structure to the driver value function. We apply the similar restriction and assume that $o_\ell(t) = \mathrm{o}(T_\ell - t, x_\ell, \Theta_\ell)$,[19] where the unobserved heterogeneity in the utility and waiting cost $(\zeta_\ell, \Theta_\ell)$ has finite support, is the same for all passengers whose origins and destinations are in the same pairs of 2 km-by-2 km square regions and is distributed independently across the pairs of regions.[20]

Below, we discuss the identification of the belief γ_ℓ and the passenger parameters. We use a maximum likelihood estimator for estimation.[21]

6.1 Identification

Belief γ_ℓ To identify the passenger belief, we require the following assumption:

Assumption 2. *Identification of Passenger Parameters*

1. $z_{k\ell} = z(route_k, T_k, route_\ell, T_\ell)$.
2. *Passenger arrival times are independent of unobserved shocks ξ_j and unobserved heterogeneity $(\zeta_\ell, \Theta_\ell)$.*

[19] The specification of the waiting cost function is explained in Online Appendix SC.

[20] Among these pairs of regions, 36% have at least 2 passenger trips, and 15% have at least 3 trips. Pairs of regions with 2 or more trips account for 63% of all passenger trips, and those with at least 3 account for 39% of all passenger trips.

[21] The likelihood function is based on passenger choice probability or hazard rate. Consider a type ℓ passenger j with a belief γ_ℓ. If the passenger j is matched at time t_j, its optimal leaving time is greater than t_j with a probability of $S_\ell(t_j;\gamma_\ell) = \frac{1}{1+\exp(o_\ell(t_j)/\gamma_\ell - v_\ell)}$. If the passenger leaves at t_j, the event is associated with the hazard rate $\left.\frac{dS_\ell(t;\gamma_\ell)}{dt}\right|_{t=t_j}$. Finally, if the passenger arrives at t_j but does not send a request, the probability is $1 - S_\ell(t_j;\gamma_\ell)$.

The first assumption states that, in the driver choice function, measures of compatibility are based on route characteristics and departure times observable to the econometrician. We thus rule out driver preferences for unobserved passenger characteristics ξ_ℓ, ζ_ℓ or Θ_ℓ. Combined with the second assumption, the decision to leave is not correlated with matching, conditional on a passenger's observed characteristics. We can thus separately identify the rates of leaving and matching (Cox, 1962). The passenger belief is identified by integrating over the instantaneous match rates.[22] We emphasize that the passenger belief is an equilibrium object and is re-computed for different market designs.

Match Preference Parameters ζ_x and ζ_f The variations in passenger characteristics identify ζ parameters in v_ℓ. Specifically, passengers with different x_ℓ or f_ℓ leave at different rates. For example, if x_ℓ is whether the starting location is in downtown, and ζ_x is positive, then passengers with downtown origins but facing the same match rate γ_ℓ are more likely to wait longer, if their other characteristics are the same.

Waiting Costs o The key variations are different passenger arrival times relative to their departure times. A similar argument that identifies the driver value function in Section 5.1.1 identifies the passenger waiting cost.

Unobserved Heterogeneity The identification of the unobserved heterogeneity also follows a similar approach to Section 5.1.1. We rely on the panel structure and the correlation of decisions to wait across passengers whose origins and destinations are in the same pair of 2 km-by-2 km square regions. The variation of beliefs γ_ℓ across passengers separately identify ζ_ℓ from Θ_ℓ.

6.2 Estimation

We use a two-step maximum likelihood estimator to estimate v_ℓ and $o_\ell(t)$. The first step estimates the belief γ_ℓ as the average of a passenger's instantaneous match rates, which in turn are estimated as a flexible function of passenger characteristics (Online Appendix SA.3). The second step uses the estimates of γ_ℓ to form the likelihood of passenger outcomes, where we integrate the joint likelihood of passengers traveling to and from the same pairs of 2 km-by-2 km square regions over the distribution of $(\zeta_\ell, \Theta_\ell)$.

Table 4 reports the estimated match preference parameters. We find that passengers traveling from downtown have a lower preference for the match. We also find substantial unobserved heterogeneity in match preferences between the two types. We note that we jointly estimate $(\zeta_\ell, \Theta_\ell)$ but only report the marginal distribution of ζ_ℓ due to the large number of parameters in the waiting cost function.

We visualize the estimated flow cost of waiting in panel (b) of Figure 5.[23] We plot the median and 25%-75% quantiles of 5-minute waiting costs over time. The median waiting costs are close to 0, although both the 25% and the 75% quantiles start to increase at around 15 minutes from the departure

[22] Appendix A Eq. (A.7) gives the exact expression for the belief.
[23] Detailed estimates are available in Online Appendix SA.5.

Table 4: Passenger Preferences for Matches

	2-Component	3-Component		2-Component	3-Component
Match Preference			Unobserved Match Preference		
Characteristics ζ_x			Component 1		
Start in Downtown	-0.28	-0.20	ζ_ℓ	-0.41	-1.65
	(0.07)	(0.07)		(0.10)	(0.14)
End in Downtown	0.05	-0.01	Prob	0.26	0.19
	(0.07)	(0.07)		(0.01)	(0.01)
Fare ζ_f	-0.12	-0.12	Component 2		
	(0.00)	(0.01)	ζ_ℓ	2.34	1.86
				(0.05)	(0.09)
			Prob	0.74	0.35
				(0.01)	(0.02)
			Component 3		
			ζ_ℓ		3.03
					(0.09)
			Prob		0.45
					(0.02)

Note: we report standard errors in parentheses.

times. A negative cost could reflect saved opportunity costs of planning alternative transports (such as delaying the need to look up bus schedules).

Passenger Types As on the driver side, the number of types and their characteristics are inputs to the simulation of the full equilibrium model in Section 4. We assume that arrival times approximate a Poisson process, which is consistent with our finding in Online Appendix SA.1. We estimate an aggregate arrival rate of 31.77 passengers/minute and use this rate to simulate the arrival times of types. Each type's route and departure time are based on the empirical distribution of these characteristics. The detailed simulation procedure is in Online Appendix SD.1.

7 Simulations

We use an iterative procedure to solve for the equilibrium in the decentralized market and under other matching policies.[24] Throughout the simulations, we assume that the fare structures do not change, because given the platform's objective to target matching between commuters, keeping a low fare is necessary to discourage the participation of professional drivers.

The first column of Table 5 presents the baseline simulation, which is based on the decentralized market.[25] The simulated number of matches and total revenue are close to those in our data (Table 1). The shares of drivers and passengers that decide to wait after arrival are also similar but slightly lower, and the average search durations are longer.

[24] We provide the details in Online Appendix SD.1.

[25] We explore the multiplicity of equilibria in Online Appendix SD.3. In general, the equilibria we find are quantitatively similar.

Table 5: Decentralized Matching and Optimal Driver Waiting

	(1) Baseline: Decentralized Matching	(2) Optimal Driver Waiting	
			Change From Baseline
Number of Matches*	405.85	406.79	0.23%
Total Revenue ($)*	1989.24	1993.53	0.22%
Δ of Average Surplus ($)**	-	0.01	-
Driver***			
% Wait After Arrival	34.62	33.03	-4.59%
Search Duration (Minutes) | Wait After Arrival	19.37	19.35	-0.09%
Search Duration (Minutes) | Matched	6.39	6.09	-4.70%
Δ of Surplus ($)	-	0.01	-
Passenger*			
% Wait After Arrival	73.46	73.47	0.01%
Search Duration (Minutes) | Wait After Arrival	6.86	6.84	-0.24%
Search Duration (Minutes) | Matched	5.83	5.81	-0.31%
Δ of Surplus ($)	-	0.01	-

*: Calculated based on passengers arriving between 4:30 pm and 5:00 pm. **: Weighted by the respective driver and passenger arrival rates. The driver arrival rate is 77.60 drivers/minute. The passenger arrival rate is 31.77 passengers/minute. ***: Calculated based on drivers with departure times between 5:00 pm and 5:20 pm.

7.1 Optimal Driver Waiting Values

When drivers cannot fully capture the passenger surplus through the distance-based fares, they may set a higher waiting value than socially optimal. We compute a counterfactual set of waiting values to maximize the social surplus. Therefore, the improvement over the decentralized market quantifies the degree of market failure.

Specifically, we choose a different $\widetilde{V}_k(t)$ in place of $V_k(t)$ in the driver choice probabilities (given in Appendix A). Then passengers form new beliefs about match rates and adjust their optimal leaving time. Our measure of social surplus is the average of driver and passenger surpluses weighted by the respective arrival rates.[26] We also note that this planner solution requires maximizing over a high dimensional space of value functions. We describe our dimension reduction technique in Online Appendix SD.4.

We find that the surplus-maximizing waiting values are \$0.77 to \$1.33 lower than those in the baseline for over 95% of drivers. The reduction is slightly larger for drivers further away from departure times. However, the overall effects on the matching outcomes are limited. Column (2) of Table 5 shows that the total number of matches increases by 0.23%. Both the driver and passenger surpluses slightly improve over the baseline.

The results show that sub-optimal driver waiting strategies have a small negative welfare effect given the decentralized market design. However, there may still exist alternative designs that further

[26] We give the exact expression in Online Appendix SD.2.

improve the market outcomes. The simulation above quantifies the potential maximum gains from modifying the waiting decision. The following two sections explore matching policies that adjust both waiting and leaving decisions.

7.2 Greedy and Patient Policies

We examine matching policies inspired by optimal algorithms in theoretical studies of centralized matching markets (Akbarpour et al., 2020; Ashlagi et al., 2023). Specifically, we focus on a "greedy" algorithm and a "patient" algorithm. In the theoretical analysis, a centralized platform has perfect knowledge of agent compatibility and attempts to match agents that leave at exogenous times. In the greedy algorithm, the platform attempts to match each arriving agent with any compatible agent waiting in the market. If no compatible match is available, the agent waits until either matching with a newly arriving compatible agent or exiting at an exogenous time. In the patient algorithm, the platform must also know each agent's exogenous leaving time. The platform then attempts to match agents just before they would exit unmatched. Compared to the greedy algorithm, this patient algorithm delays matches, which increases market thickness and thus matching probability.

We adapt these algorithms to our decentralized setting, where the platform does not have prefect knowledge of agent preferences or when they would leave endogenously. Under our greedy policy, a driver upon arrive must decide whether to choose a passenger or leave immediately. The passengers respond to the driver side change by adjusting beliefs and optimal leaving times. The policy is equivalent to setting the driver waiting value to $-\infty$ in the planner solution in Section 7.1. Although the results there show that the scope for surplus improvement may be limited, the policy could nonetheless increase the number of matches.

Next, we examine a patient matching policy based on the reported trip departure times. Specifically, when a driver arrives at the platform, she can choose a passenger, continue to wait or leave the platform. Should she choose to continue to wait, the driver's choice is more limited: at every move, she can choose from the observed passengers or wait. The driver cannot leave the market without a match until reaching her departure time. Similarly, an arriving passenger must either leave the platform or agree to wait. A waiting passenger must also commit to waiting until being matched or reaching the departure time. We describe the agent strategies and equilibrium conditions under the patient policy in Appendix A.4.

Why might this policy increase the number of matches or improve efficiency? The key idea is that, despite being unable to predict unmatched exits, the platform may still benefit by reducing them. For any waiting driver, matching becomes more likely when leaving is restricted. For any waiting passenger, the policy could increase their search durations, thus thickening the market and improving the probability of matching. However, banning unmatched exits could lower the waiting values for arriving drivers and passengers, reducing their willingness to participate. The overall effect of the policy depends on the tradeoff between the increased probability of matching among waiting agents and the potential decline in market participation.

Table 6 presents the results from these counterfactual simulations. Column (1) shows that the greedy policy increases the number of matches slightly but reduces the total revenue. The main reason

Table 6: Greedy and Patient Policies

	(1) Greedy		(2) Patient		(3) Driver-only Patient		(4) Passenger-only Patient	
		Change From Baseline		Change From Baseline		Change From Baseline		Change From Baseline
Number of Matches*	406.65	0.20%	496.17	22.26%	488.95	20.48%	413.66	1.93%
Total Revenue ($)*	1988.32	-0.05%	2379.02	19.59%	2351.78	18.22%	2021.76	1.63%
Δ of Average Surplus ($)**	-3.43	-	-1.77	-	-1.62	-	-0.17	-
Driver***								
% Wait After Arrival	0.00	-100.00%	21.16	-38.86%	21.14	-38.92%	34.61	-0.03%
Search Duration (Minutes) | Wait After Arrival	-	-	23.32	20.41%	23.32	20.39%	19.38	0.08%
Search Duration (Minutes) | Matched	-	-	6.94	8.54%	6.94	8.51%	6.41	0.31%
Δ of Surplus ($)	-4.56	-	-2.57	-	-2.61	-	0.04	-
Passenger*								
% Wait After Arrival	72.36	-1.50%	59.26	-19.32%	77.28	5.20%	52.74	-28.21%
Search Duration (Minutes) | Wait After Arrival	6.66	-2.94%	6.75	-1.57%	6.28	-8.43%	7.47	8.91%
Search Duration (Minutes) | Matched	5.63	-3.52%	6.16	5.64%	5.35	-8.25%	6.85	17.45%
Δ of Surplus ($)	-0.13	-	0.59	-	1.29	-	-0.80	-

*: Calculated based on passengers arriving between 4:30 pm and 5:00 pm. **: Weighted by the respective driver and passenger arrival rates. The driver arrival rate is 77.60 drivers/minute. The passenger arrival rate is 31.77 passengers/minute. ***: Calculated based on drivers with departure times between 5:00 pm and 5:20 pm.

is that matches are shifted towards shorter trips from or to downtown. Given the higher downtown passenger arrival rates, it is relatively easier for drivers in the same locations to find compatible matches. Banning waiting reduces driver surplus. The passenger surplus also falls because of the change in the composition of matches, despite the policy increasing the number of matches.

The patient policy achieves a much larger increase in the number of matches and revenue (Column (2) in Table 6), but average surplus and market thickness decrease. Overall, driver surplus decreases by \$2.85, about 60% of the average fare. In comparison, the passenger surplus increases slightly. The percentage of drivers who wait after arrival (as opposed to leaving or choosing a passenger) decreases from 34.62% in the decentralized market to 21.16%. We also find that the vast majority of drivers that decide not to wait after arrival choose to leave immediately (85%) as opposed to matching with a passenger. The remaining drivers spend 20.41% more time searching. We observe a similar pattern on the passenger side. The market thickness is lower, because participation rates fall more proportionally than search durations. Interestingly, the total passenger search duration conditional on waiting decreases, even though the search time conditional on being matched increases. The result reflects a change in the composition of waiting passengers, who now consist of more passengers arriving closer to their departure times.

Decomposing the Effects of the Patient Policy

We focus on the patient policy given its large effects compared with the greedy policy. We ask: does the patient policy affect drivers or passengers more? We compare a driver-only and a passenger-only patient policy. Under the driver-only patient policy, only the arriving drivers are asked to match, leave or commit to waiting and searching. Any waiting passenger is free to leave as in the decentralized market. Similarly, the passenger-only patient policy is enforced only on passengers.

We report the two results in Columns (3) and (4) of Table 6 . We find that a driver-only patient policy achieves 92% of the increase in the number of matches under the full patient policy. In the new equilibrium, passengers adjust their beliefs in response to the increased match rates and are more likely to wait after arrival. A passenger-only policy has a similar effect on drivers, although the magnitude is much smaller.

A Hybrid Policy

Our next exercise focuses on adjusting driver behaviors given the large effect of the driver-only patient policy. The analysis above shows that reducing the driver waiting values and banning their unmatched exits can increase the number of matches, but the ban reduces participation and surplus. We thus ask: can a matching policy reduce the value of waiting but also lessen the burden of the patient policy?

We thus consider a design that combines the greedy and patient policies. Specifically, a hybrid policy sets a deadline $t_k < T_k$ for a type k driver. An arriving driver can choose between matching, leaving or agreeing to the following shorter commitment: the driver can wait and match with a passenger before t_k, but cannot leave without a match; an unmatched driver reaching t_k must leave immediately.

Table 7: Best Hybrid Policy

			Change From Baseline
Number of Matches*		428.35	5.54%
Total Revenue ($)*		2086.72	4.90%
Δ of Average Surplus ($)**		0.05	-
Driver***			
	% Wait After Arrival	34.56	-0.17%
	Search Duration (Minutes) | Wait After Arrival	15.95	-17.64%
	Search Duration (Minutes) | Matched	5.31	-16.89%
	Δ of Surplus ($)	-0.03	-
Passenger*			
	% Wait After Arrival	74.72	1.72%
	Search Duration (Minutes) | Wait After Arrival	6.74	-1.75%
	Search Duration (Minutes) | Matched	5.75	-1.31%
	Δ of Surplus ($)	0.29	-

*: Calculated based on passengers arriving between 4:30 pm and 5:00 pm. **: Weighted by the respective driver and passenger arrival rates. The driver arrival rate is 77.60 drivers/minute. The passenger arrival rate is 31.77 passengers/minute. ***: Calculated based on drivers with departure times between 5:00 pm and 5:20 pm.

We consider deadlines of $t_k = 5, 10, \ldots$ minutes after arrival. The greedy policy corresponds with $t_k = 0$, while the patient policy corresponds with $t_k = T_k$. We also include two additional restrictions. First, we exclude drivers whose departure time is too imminent. Specifically, drivers are subject to the policy only if their arrival times are more than 5 minutes before the departure time. The exclusion ensures that the policy does not force these drivers to incur high waiting costs. Second, we exclude drivers whose departure times are significantly later than their arrival times. In Online Appendix SA.6, we show that most drivers do not frequently check their phones until close to the departure times. To ensure that drivers check their phones with a sufficiently high probability when the deadline arrives, we apply the policy to drivers whose departure times are within 10 minutes from the deadline.[27]

We find that at $t_k = 5$, both the net surplus and the total number of matches increase. Specifically, this hybrid policy applies to drivers who arrive between 15 and 10 minutes before the departure time. These drivers are then given 5 minutes to search. We report the effects in Table 7. Relative to the decentralized market, a slightly smaller number of drivers decide to wait, and their search durations decrease. More passengers participate in matching, and their search durations fall as well. Despite a small loss of driver surplus, the passenger surplus increases sufficiently that the average surplus improves.

[27] We assume that the move arrival rates do not change under this policy. If drivers instead check the passengers more often in response to the deadline, we find that the number of matches would increase more.

7.3 Discussion

Limitations

We note three limitations of our exercises. First, although we endogenize driver and passenger decisions to wait upon arrival, we assume their arrival decisions are exogenous. In particular, when agents' expected surplus falls, fewer may choose to open the app entirely. To understand the sensitivity of our results, we can simulate the policy effects with different arrival rates. We find that, for example, the driver arrival rate needs to decrease by 20% to reverse the gains in the number of matches under the driver-only patient policy.[28]

A second limitation is that agents may strategically misreport a more imminent departure time to "escape" the commitment under the patient policy. Under the driver-only patient policy, misreporting removes the commitment before the actual departure time. We find that driver commitment that lasts as little as 5 minutes can increase the total number of matches 4.44%, but the total surplus falls. In contrast, the hybrid policy combines the commitment with the requirement to leave after waiting 5 minutes, which adds more matches and achieves a net increase in surplus.

Furthermore, requiring drivers to search poses several challenges for implementation. First, a driver may participate in the matching nominally. Namely, after agreeing to wait but deciding to leave anyway, a driver may still keep the app open but just start her trip. To address this issue, the platform can geo-locate a driver's phone to ensure that the driver remains in the same location. We note that geo-location is an essential and uncontroversial part of almost all ride-hailing apps. In addition, the app can send periodic reminders to prompt the drivers to view the set of waiting passengers. The platform can also require a driver to view the list at least once per 5 minutes as part of the commitment. Second, a driver may simply decide to close the app and stop the search even after agreeing to wait after arrival. A direct solution is to temporarily suspend the driver from using the platform for violations. In general, limiting usage is a common way for ride-hailing platforms to enforce control.[29] On the other hand, it is also common for ride-hailing platforms to reward more active drivers, such as the Uber Pro and Lyft Rewards programs. The carpooling platform can similarly offer additional (fixed-sum) pay to drivers for complying with the market design. We note that the platform we study is in a unique position to enforce these rules. Both the carpooling platform and the ride-hailing platform are dominant in the local market. The company can thus leverage cross-platform incentives and penalties for policy implementation.

Extension

Our simulations above examine market designs that adjust agent decisions to wait and leave. We also consider a design that directly influences driver decisions to match by modifying the set of potential

[28] Agents whose surplus falls more are more likely to stop using the app. Under the patient or the driver-only patient policies, the surplus decreases more for drivers that arrive earliest relative to the departure times. The hybrid policy avoids this surplus loss by targeting drivers that arrive closer to the departure time.

[29] A nontrivial share of drivers routinely use this carpooling platform, and limiting usage could be a sufficient deterrence. In our 20-day sample, 34% of drivers search for passengers the platform on at least two different days. On Lyft, for example, a driver may lose "driving priority", the priority for receiving orders, if a driver declines requests too many times (Lyft (2019, 2023)). Uber sends out fewer requests to drivers who declines rides (Marshall (2020)).

passengers available to a driver. As motivation, we note that common ride-hailing platforms such as Uber or Lyft sequentially offer rides to a driver instead of allowing drivers to choose from a list. We do not consider this specific design, which alters how drivers browse the list of passengers and can cause changes beyond our model. Instead, we consider making passengers selectively visible to drivers. In the current decentralized market, a driver can see all waiting passengers. Alternatively, the platform can show the driver just a subset of these passengers. On one hand, reducing driver choice set affects the value of waiting and could incentivize faster matching. On the other hand, a smaller choice set decreases the probability of a driver finding a compatible match. On net, we find that hiding passengers from a driver generally decreases probabilities of matching and surpluses.[30]

8 Conclusion

The success of online platforms often rely heavily on the use of vast amounts of personal consumer data (Brynjolfsson and McElheran, 2016; Goldfarb and Tucker, 2019). With increasing privacy concerns (Fainmesser et al., 2023), governments around the world responded with new laws[31] that require firms to use less information when designing platform strategies.

Our work evaluates whether matching policies based on limited information reported by consumers can improve matching outcomes. These policies do not force matches but adjust the decisions to wait or leave. We simulate the effects of these policies in a dynamic matching model of a carpooling platform estimated based on driver and passenger choices in the data. Our results show that such polices can have large effects on surplus and the number of matches.

Lastly, we note that our matching market and other similar carpooling platforms like BlaBlaCar are of independent interests as alternatives to common ride-hailing platforms. Past research has found that ride-hailing platforms often increase congestion and air pollution (Barnes, Guo and Borgo, 2020; Diao, Kong and Zhao, 2021; Tarduno, 2021), as many people join the platform as new full-time drivers (Chen, Rossi, Chevalier and Oehlsen, 2019). Our carpooling platform aims to increase car occupancy rates of existing car-driving commuters, which may lead to a more sustainable solution to urban transportation. However, commonly used tools to improve matching efficiency such as dynamic pricing may not be feasible, because prices need to be kept sufficiently low to keep out professional drivers. This setting thus presents a unique opportunity for considering new market designs.

References

Abbring, Jaap H and Øystein Daljord, "Identifying the discount factor in dynamic discrete choice models," *Quantitative Economics*, 2020, *11* (2), 471–501.

[30] Online Appendix SE describes simulations of a policy where a "visibility probability" determines how often a passenger is visible to a driver based on observed characteristics, and we choose these probabilities to maximize the number of matches or average surplus.

[31] Examples include the General Data Protection Regulation (GDPR) in Europe, the California Consumer Privacy Act (CCPA) in the US, and the Personal Information Protection Law (PIPL) in China.

Agarwal, Nikhil and Eric Budish, "Market design," *Handbook of Industrial Organization*, 2021, *5* (1), 1–79.

_ , Itai Ashlagi, Michael A Rees, Paulo Somaini, and Daniel Waldinger, "Equilibrium allocations under alternative waitlist designs: Evidence from deceased donor kidneys," *Econometrica*, 2021, *89* (1), 37–76.

Akbarpour, Mohammad, Shengwu Li, and Shayan Oveis Gharan, "Thickness and information in dynamic matching markets," *Journal of Political Economy*, 2020, *128* (3), 783–815.

Ashlagi, Itai, Afshin Nikzad, and Philipp Strack, "Matching in dynamic imbalanced markets," *The Review of Economic Studies*, 2023, *90* (3), 1084–1124.

_ , Maximilien Burq, Patrick Jaillet, and Vahideh Manshadi, "On matching and thickness in heterogeneous dynamic markets," *Operations Research*, 2019, *67* (4), 927–949.

Baccara, Mariagiovanna, SangMok Lee, and Leeat Yariv, "Optimal dynamic matching," *Theoretical Economics*, 2020, *15* (3), 1221–1278.

Bajari, Patrick, C Lanier Benkard, and Jonathan Levin, "Estimating dynamic models of imperfect competition," *Econometrica*, 2007, *75* (5), 1331–1370.

Barnes, Stuart J, Yue Guo, and Rita Borgo, "Sharing the air: Transient impacts of ride-hailing introduction on pollution in China," *Transportation Research Part D: Transport and Environment*, 2020, *86*, 102434.

Berry, Steven T and Philip A Haile, "Identification in differentiated products markets using market level data," *Econometrica*, 2014, *82* (5), 1749–1797.

Bian, Bo, "Search frictions, network effects and spatial competition: taxis versus Uber," Technical Report, mimeo, Penn State University 2020.

Bimpikis, Kostas, Wedad J Elmaghraby, Ken Moon, and Wenchang Zhang, "Managing market thickness in online business-to-business markets," *Management Science*, 2020, *66* (12), 5783–5822.

BlaBlaCar, "How Pricing Works," 2024. Accessed: 2024-10-04.

Brancaccio, Giulia, Myrto Kalouptsidi, and Theodore Papageorgiou, "Geography, transportation, and endogenous trade costs," *Econometrica*, 2020, *88* (2), 657–691.

_ , _ , _ , and Nicola Rosaia, "Search frictions and efficiency in decentralized transport markets," *Quarterly Journal of Economics*, 2023, *138* (4), 2451–2503.

Brynjolfsson, Erik and Kristina McElheran, "The rapid adoption of data-driven decision-making," *American Economic Review*, 2016, *106* (5), 133–139.

Buchholz, Nicholas, "Spatial equilibrium, search frictions, and dynamic efficiency in the taxi industry," *Review of Economic Studies*, 2022, *89* (2), 556–591.

Castillo, Juan Camilo, "Who Benefits from Surge Pricing?," *Available at SSRN 3245533*, 2020.

Chen, M Keith, Peter E Rossi, Judith A Chevalier, and Emily Oehlsen, "The value of flexible work: Evidence from uber drivers," *Journal of Political Economy*, 2019, *127* (6), 2735–2794.

Chen, Yan, "Matching market experiments," in Federico Echenique, Nicole Immorlica, and Vijay V. Vazirani, eds., *Online and Matching-Based Market Design*, Cambridge University Press, 2023.

_ , **Peter Cramton, John A List, and Axel Ockenfels**, "Market design, human behavior, and management," *Management Science*, 2021, *67* (9), 5317–5348.

China Daily, "2023 social value report of the ridesharing industry," 2023.

Cox, David Roxbee, "Renewal theory," *Chapman and Hall*, 1962.

Cullen, Zoë and Chiara Farronato, "Outsourcing tasks online: Matching supply and demand on peer-to-peer internet platforms," *Management Science*, 2020.

Diao, Mi, Hui Kong, and Jinhua Zhao, "Impacts of transportation network companies on urban mobility," *Nature Sustainability*, 2021, *4* (6), 494–500.

Doval, Laura, "Dynamically stable matching," *Theoretical Economics*, 2022, *17* (2), 687–724.

Einav, Liran, Chiara Farronato, and Jonathan Levin, "Peer-to-peer markets," *Annual Review of Economics*, 2016, *8*, 615–635.

Ericson, Richard and Ariel Pakes, "Markov-perfect industry dynamics: A framework for empirical work," *Review of Economic Studies*, 1995, *62* (1), 53–82.

Fainmesser, Itay P, Andrea Galeotti, and Ruslan Momot, "Digital privacy," *Management Science*, 2023, *69* (6), 3157–3173.

Farronato, Chiara and Andrey Fradkin, "The welfare effects of peer entry: the case of Airbnb and the accommodation industry," *American Economic Review*, 2022, *112* (6), 1782–1817.

Fong, Jessica, "Effects of market size and competition in two-sided markets: Evidence from online dating," *Marketing Science*, 2024.

Frechette, Guillaume R, Alessandro Lizzeri, and Tobias Salz, "Frictions in a competitive, regulated market: evidence from taxis," *American Economic Review*, 2019, *109* (8), 2954–92.

Gaineddenova, Renata, "Pricing and efficiency in a decentralized ride-hailing platform," 2022.

Goldfarb, Avi and Catherine Tucker, "Digital economics," *Journal of Economic Literature*, 2019, *57* (1), 3–43.

_ **and Verina F Que**, "The economics of digital privacy," *Annual Review of Economics*, 2023, *15* (1), 267–286.

Hitsch, Gunter J, Ali Hortaçsu, and Dan Ariely, "Matching and sorting in online dating," *American Economic Review*, 2010, *100* (1), 130–63.

Hotz, V Joseph and Robert A Miller, "Conditional choice probabilities and the estimation of dynamic models," *Review of Economic Studies*, 1993, *60* (3), 497–529.

Jullien, Bruno, Alessandro Pavan, and Marc Rysman, "Two-sided markets, pricing, and network effects," in "Handbook of Industrial Organization," Vol. 4, Elsevier, 2021, pp. 485–592.

Kasahara, Hiroyuki and Katsumi Shimotsu, "Nonparametric identification of finite mixture models of dynamic discrete choices," *Econometrica*, 2009, *77* (1), 135–175.

Lagos, Ricardo, "An analysis of the market for taxicab rides in New York City," *International Economic Review*, 2003, *44* (2), 423–434.

Lewbel, Arthur, "An overview of the special regressor method," 2014.

_ , "The identification zoo: Meanings of identification in econometrics," *Journal of Economic Literature*, 2019, *57* (4), 835–903.

Li, Jun and Serguei Netessine, "Higher market thickness reduces matching rate in online platforms: Evidence from a quasiexperiment," *Management Science*, 2020, *66* (1), 271–289.

Liu, Xi, Li Gong, Yongxi Gong, and Yu Liu, "Revealing travel patterns and city structure with taxi trip data," *Journal of Transport Geography*, 2015, *43*, 78–90.

Loertscher, Simon, Ellen V Muir, and Peter G Taylor, "Optimal market thickness," *Journal of Economic Theory*, 2022, *200*, 105383.

Lyft, "What the New TLC Rules Mean for You," https://www.lyft.com/hub/posts/what-the-new-tlc-rules-mean-for-you 2019.

_ , "Acceptance rate," https://help.lyft.com/hc/lt/all/articles/115013077708-Acceptance-rate 2023.

Magnac, Thierry and David Thesmar, "Identifying dynamic discrete decision processes," *Econometrica*, 2002, *70* (2), 801–816.

Manski, Charles F, "Identification of binary response models," *Journal of the American statistical Association*, 1988, *83* (403), 729–738.

Marshall, Aarian, "Uber Changes Its Rules, and Drivers Adjust Their Strategies," *WIRED*, Feb 2020.

Ostrovsky, Michael and Michael Schwarz, "Carpooling and the Economics of Self-Driving Cars," 2018.

Piketty, Thomas, Li Yang, and Gabriel Zucman, "Capital accumulation, private property, and rising inequality in China, 1978–2015," *American Economic Review*, 2019, *109* (7), 2469–2496.

Reeling, Carson and Valentin Verdier, "Welfare effects of dynamic matching: An empirical analysis," *Review of Economic Studies*, 2021.

Romanyuk, Gleb and Alex Smolin, "Cream skimming and information design in matching markets," *American Economic Journal: Microeconomics*, 2019, *11* (2), 250–276.

Rosaia, Nicola, "Competing platforms and transport equilibrium: evidence from New York City," Technical Report, mimeo, Harvard University 2020.

Roth, Alvin E, "Experiments in market design," *Handbook of Experimental Economics*, 2016, *2*, 290–346.

Rust, John, "Structural estimation of Markov decision processes," *Handbook of Econometrics*, 1994, *4*, 3081–3143.

Rysman, Marc, "The economics of two-sided markets," *Journal of Economic Perspectives*, 2009, *23* (3), 125–143.

Schäfer, Uwe, *From Sperner's Lemma to Differential Equations in Banach Spaces: An Introduction to Fixed Point Theorems and Their Applications*, KIT Scientific Publishing, 2014.

Shapiro, Matthew H, "Density of demand and the benefit of Uber," 2018.

Tarduno, Matthew, "The congestion costs of Uber and Lyft," *Journal of Urban Economics*, 2021, *122*, 103318.

Waldinger, Daniel, "Targeting in-kind transfers through market design: A revealed preference analysis of public housing allocation," *American Economic Review*, 2021, *111* (8), 2660–96.

A Matching Equilibrium

A.1 Driver Decisions

For driver beliefs, we use $p_k(t)$ to denote the probability that the observed set of passengers $\mathfrak{S}_t$ is non-empty at t. The driver also forms a belief about the highest passenger value (net of the EV1 shock) $\max_{j\in\mathfrak{S}_t} u_{ij}$. We use $G_k(u;t)$ to denote, conditional on $\mathfrak{S}_t \neq \emptyset$, the distribution of u at time t. We also use $g_{k\ell}(u;t)$ to denote the probability that a type ℓ passenger with match value u is the highest value passenger conditional on $\mathfrak{S}_t \neq \emptyset$.

For driver choice probabilities, we first consider drivers who decide to wait upon arrival. Conditional on a move at t, the probability $q_{k\ell}(t)$ that a type k driver matches with a type ℓ passenger

when this passenger is observed is

$$q_{k\ell}(t) = p_k(t) \int \frac{\exp(u)}{\exp(u) + \exp(V_k(t)) + 1} g_{k\ell}(u;t)\, \phi\left(\frac{u - u_{k\ell}}{\sigma}\right) / \sigma du. \tag{A.1}$$

The probability of a driver leaving the market without a match is:

$$w_k(t) = p_k(t) \int \frac{1}{\exp(u) + \exp(V_k(t)) + 1} dG_k(u;t) + (1 - p_k(t)) \frac{1}{\exp(V_k(t)) + 1}. \tag{A.2}$$

A.2 Passenger Decisions

The probability S_ℓ that a type ℓ passenger sets an optimal leaving time after t is defined in Eq. (3). The leaving rate at t is

$$r_\ell(t) = \frac{dS_\ell}{dt}. \tag{A.3}$$

A.3 Matching Equilibrium

We use t_k^0 to denote the earliest arrival time of type k drivers. To ensure equilibrium existence, we assume that the arrival time of type k drivers follows a continuous density η_k, where $\int_{t_k^0}^{T_k} \eta_k = 1$. The density smoothes the mass transition process in the equilibrium. In principle, the density can be "steep" near t_k^0 and nearly 0 anywhere else to approximate that all type k drivers arrive at t_k^0.

The type ℓ passenger arrival and departure times are t_ℓ^0 and T_ℓ. We assume that a unit mass of type ℓ passengers arrives at t_ℓ^0.[32] We also assume that, for any type ℓ passenger, there exists at least one driver type k such that $[t_\ell^0, T_\ell]$ and $[t_k^0, T_k]$ overlap.

To tractably define equilibrium beliefs, we use the following assumption:

Assumption 3. *(Driver Choice Set) At time t, a driver observes one passenger of type ℓ with probability $n_\ell(t)$ independently.*

Specifically, we assume that the set of passengers a driver observes is composed of at most one passenger per type. The probability that a type ℓ passenger is in this set is $n_\ell(t)$. This assumption is a key part of our equilibrium notion. An important benefit of this assumption is that consistent driver beliefs now have simple forms. As an example, suppose $n_1(t) = \frac{1}{4}$ and $n_2(t) = \frac{1}{3}$. Then the possible sets of passengers a driver searching at t are

$$\{\emptyset\}, \{\text{a type 1 passenger}\}, \{\text{a type 2 passenger}\}, \{\text{a type 1 passenger and a type 2 passenger}\}.$$

The probabilities for these outcomes are $\frac{3}{4} \cdot \frac{2}{3}, \frac{1}{4} \cdot \frac{2}{3}, \frac{3}{4} \cdot \frac{1}{3}$ and $\frac{1}{4} \cdot \frac{1}{3}$.

Given the assumption above, the probability of observing a non-empty set for a type k driver is

$$p_k(t) = 1 - \prod_\ell (1 - n_\ell(t)). \tag{A.4}$$

[32] We could alternatively allow passengers to also arrive gradually between t_ℓ^0 and T_ℓ accordingly to some continuous density.

For $g_{k\ell}$, if the driver value for matching with a type ℓ passenger is u, then the probability that the driver prefers this passenger to another type ℓ' passenger is $\Phi\left(\frac{u-u_{k\ell'}}{\sigma}\right)$. Therefore the probability that the driver prefers this passenger to any other passenger is

$$g_{k\ell}(u;t) = n_\ell(t) \cdot \prod_{\ell' \neq \ell} \left(n_{\ell'}(t) \cdot \Phi\left(\frac{u-u_{k\ell'}}{\sigma}\right) + 1 - n_{\ell'}(t) \right), \tag{A.5}$$

where $1-n_{\ell'}(t)$ is the probability that the type ℓ' passenger is not in the choice set. Hence the density function $g_k(u;t)$ of $G_k(u;t)$ is

$$g_k(u;t) = \frac{\sum_\ell g_{k\ell}(u;t)\,\phi\left(\frac{u-u_{k\ell}}{\sigma}\right)/\sigma}{p_k(t)}, \tag{A.6}$$

where ϕ is the standard normal density.

For passengers, we define the passenger belief as the average type ℓ match rate:

$$\gamma_\ell = \frac{1}{T_\ell - t_\ell^0} \left(\int_{t_\ell^0}^{T_\ell} \sum_{k=1}^{K} (\eta_k + \lambda_k m_k)\, q_{k\ell} dt \right). \tag{A.7}$$

The equilibrium places three sets of restrictions on $\{V_k, q_{k\ell}, w_k, S_\ell, r_\ell, p_k, g_{k\ell}, G_k, \gamma_\ell, m_k, n_\ell\}$.

1. (Optimality conditions) The driver value functions and choice probabilities are given in (1), (A.1) and (A.2). The passenger leaving rate is given by (A.3).

2. (Consistent beliefs) The driver beliefs $(p_k, g_{k\ell}, G_k)$ are consistent with (A.4), (A.5) and (A.6); the passenger belief of the average match rate is consistent with (A.7).

3. (Mass transitions) The driver mass $m_k(t)$ is 0 for $t \notin [t_k^0, T_k]$. For $t \in [t_k^0, T_k]$,(omitting the argument of t)
$$\frac{dm_k}{dt} = \eta_k - (\eta_k + \lambda_k m_k) \cdot \left(\sum_\ell n_\ell q_{k\ell} + w_k \right), \tag{A.8}$$
with the boundary condition $m_k(t_k^0) = 0$. For passengers, the mass $n_\ell(t) = 0$ for $t \notin [t_\ell^0, T_\ell]$. For $t \in [t_\ell^0, T_\ell]$,
$$\frac{dn_\ell}{dt} = -n_\ell \left(\sum_k (\eta_k + \lambda_k m_k)\, q_{k\ell} + r_\ell \right), \tag{A.9}$$
with the boundary condition $n_\ell(t_\ell^0) = S_\ell(t_\ell^0; \gamma_\ell)$.

To establish equilibrium existence, we note that the passenger belief γ_ℓ is bounded strictly above 0 given the overlap condition at the beginning of this subsection. Therefore every passenger type has a positive mass over $[t_\ell^0, T_\ell]$. In addition, we note that the agent masses, value functions and choice probabilities are all continuous functions. Then we can apply the Schauder Fixed Point Theorem (Schäfer, 2014) to show the existence.

A.4 Matching Equilibrium Under Patient Policies

For brevity, we define the equilibrium for the full patient policy. The driver-only, passenger-only or the hybrid policy equilibrium can be defined analogously.

For a type k driver that just arrives at t, the probability of choosing a type ℓ passenger is given by

$$q_{k\ell}^{0}(t) = p_k(t) \int \frac{\exp(u)\, g_{k\ell}(u;t)\, \phi\left(\frac{u-u_{k\ell}}{\sigma}\right)/\sigma}{\exp(u)+\exp(V_k(t))+1} du, \tag{A.10}$$

and the probability of leaving is

$$w_k^0(t) = p_k(t) \int \frac{1}{\exp(u)+\exp(V_k(t))+1} dG_k(u;t) + (1-p_k(t)) \frac{1}{\exp(V_k(t))+1}.$$

A waiting driver does not leave without a match. The probability of choosing a type ℓ passenger is

$$q_{k\ell}(t) = p_k(t) \int \left(\frac{\exp(u)}{\exp(u)+\exp(V_k(t))}\right) g_{k\ell}(u;t)\, \phi\left(\frac{u-u_{k\ell}}{\sigma}\right)/\sigma du. \tag{A.11}$$

For passengers under the patient policy, the value function upon arrival is

$$\overline{W}_j^0 = \max\left\{ v_{0j}, \int_{t_j^0}^{T_\ell} \gamma_\ell (v_j - o_\ell(\tau)) \exp\left(-\gamma_\ell\left(\tau - t_j^0\right)\right) d\tau \right\}. \tag{A.12}$$

The implied probability that a type ℓ passenger arriving at t_ℓ^0 will send a request and wait is $\overline{S}_\ell\left(t_\ell^0;\gamma_\ell\right)$:

$$\overline{S}_\ell\left(t_\ell^0;\gamma_\ell\right) = \exp\left(v_\ell - \overline{v}_\ell\left(t_\ell^0\right)\right) / \left(1+\exp\left(v_\ell - \overline{v}_\ell\left(t_\ell^0\right)\right)\right), \tag{A.13}$$

where

$$\overline{v}_\ell\left(t_\ell^0\right) = \frac{\int_{t_\ell^0}^{T_\ell} \gamma_\ell o_\ell(\tau) \exp\left(-\gamma_\ell\left(\tau - t_\ell^0\right)\right) d\tau}{1-\exp\left(-\gamma_\ell\left(T_\ell - t_\ell^0\right)\right)}.$$

The agent beliefs are similarly defined as in Appendix A.3. The mass transition functions are modified as

$$\frac{dm_k}{dt} = \eta_k\left(1-w_k^0\right) - \left(\eta_k + \lambda_k m_k\right) \cdot \sum_\ell n_\ell q_{k\ell}, \tag{A.14}$$

with the boundary condition $m_k\left(t_k^0\right) = 0$. For passengers,

$$\frac{dn_\ell}{dt} = -n_\ell\left(\sum_k \lambda_k m_k q_{k\ell} + \sum_k \eta_k q_{k\ell}^0\right), \tag{A.15}$$

with the boundary condition $n_\ell\left(t_\ell^0\right) = \overline{S}_\ell\left(t_\ell^0;\gamma_\ell\right)$. The masses are set to 0 outside $\left[t_k^0, T_k\right]$ and $\left[t_\ell^0, T_\ell\right]$.

Figure SA.1. Number of Passenger Arrivals Per Minute

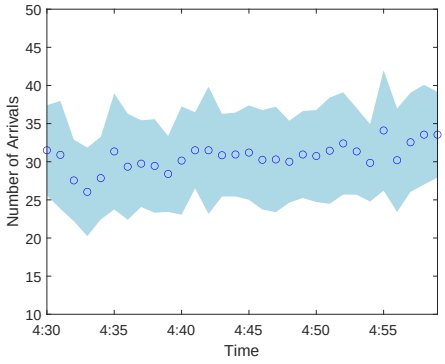

Note: the color fill indicates 95% confidence intervals based on the number of arrivals in each minute across 20 days in the data.

SA Additional Estimates

SA.1 Passenger Arrival Rate

In Figure SA.1, we plot the average number of passenger arrivals per minute from 4:30 pm to 5:00 pm averaged across the 20 days in our data. The arrival rate is 31.77 passengers / minute.

SA.2 Dyadic Regressions

We estimate the effects of compatibility measures and time-to-departure on matching using dyadic regressions. Each driver search instance corresponds with a maximum of 85 passengers sorted by the compatibility score. For each dyad, we regress the indicator of whether the driver matches with the passenger on measures of compatibility, driver characteristics and driver waiting time. Specifically, we use $y_{ijt} = 1$ to denote a match between driver i and passenger j at time t. The linear probability model we estimate is

$$\begin{aligned} y_{ijt} = {} & \alpha_z z_{ij} + \alpha_f f_j + \alpha_x x_i + \alpha_{30} \mathbb{1}\left(T_i - t < 30\right) + \alpha_{20} \mathbb{1}\left(T_i - t < 20\right) \\ & + \alpha_{10} \mathbb{1}\left(T_i - t < 10\right) + \alpha_0 + \text{unobservables}, \end{aligned}$$

where z_{ij} is a vector of the compatibility measures, including the compatibility score, pickup and dropoff distances and differences in departure times, f_j is the fare of the request and x_i consists of driver characteristics, including trip lengths and whether it starts or ends in downtown. The parameters $\alpha_{30}, \alpha_{20}, \alpha_{10}$ measure the change in the probability of matching when the driver is within 30, 20, and 10 minutes from the departure time. The regression results are presented in Table SA.1. The estimates are in percentage point terms (multiplied by 100). We find that a 10 percentage-point increase in compatibility scores is associated with up to 0.177 percentage point increase in match probability. This effect is large, given that the mean probability of matching with a passenger in

the dyadic sample is 0.16%. The estimates of other covariates on measures of compatibility are also intuitive. Furthermore, the regression shows that a driver closer to the departure time is more likely to match with a passenger. These findings are consistent with our interviews of drivers.

SA.3 Estimated Passenger Match Rates

To flexibly estimate the match rates, we discretize time into 30-second intervals and specify the probability that the passenger is matched in the next period as a logit function of a vector of covariates that include a constant, fare, fare's square, whether the trip starts in downtown, whether the trip ends in downtown, whether the distance is between 10 to 30 km, whether the distance is greater than 30 km, whether the stated departure time is between 20 to 30 minutes later after arrival, and whether the departure time is more than 30 minutes after arrival. We allow the coefficients to vary across each 30-second interval by separately estimating this logit probability function for each period after arrival via maximum likelihood. The sample for each period consists of all passengers who are in the market at the beginning of the period. Let j denote a passenger and $\mathfrak{t}$ index a period, which is $\Delta^{\text{psg}} = 0.5$ minutes long. Given the arrival time t_j^0 and departure time T_j, the total number of periods for the passenger is $\mathfrak{T}_j = \left\lceil \frac{T_j - t_j^0}{\Delta^{\text{psg}}} \right\rceil$, where $\lceil \cdot \rceil$ denotes the function to round up to the nearest integer. Let $\mathfrak{p}_{j\mathfrak{t}}$ denote the estimated match probability. Figure SA.2.(a) shows the estimated match probabilities $\mathfrak{p}_{j\mathfrak{t}}$ as time approaches the departure time. The black lines represent the 25% and 75% quantiles across passengers and reflect the dispersion of this probability for different passengers, and the blue line represents the median.[33] Panel (b) plots the histogram of the passenger beliefs, which is the average probability of match in every 30 seconds:

$$\gamma_j = \frac{1}{\mathfrak{T}_j} \sum_{\mathfrak{t}=1}^{\mathfrak{T}_j} \mathfrak{p}_{j\mathfrak{t}}. \tag{SA.1}$$

SA.4 Simulate Passengers That Arrive Before 4:30 pm or After 5:00 pm in the Driver Choice Set

We assume that the arrival times of passengers approximate a Poisson process at the estimated rate of 31.77 passengers/minute from 4:00 pm to 6:00 pm. We also assume that routes and departure times are independently distributed conditional on the arrival time. We therefore simulate the routes and departure times using the respective empirical distributions. For each type, we draw the unobserved heterogeneity independently from the estimated distributions in Section 6 for each pair of 2km-by-2km square regions containing the origins and destinations of the trips. We then compute the belief of the average match rate in (SA.1) using estimates of the match probability based on passenger characteristics in Appendix SA.3. The discretized passenger mass transitions follow Appendix SD.1.2. We use $\mathfrak{t}$ to index a period and $n_{j\mathfrak{t}}$ to denote the mass of a passenger type in a period $\mathfrak{t}$. For each driver that searches at the clock time t, the set of passengers that the driver sees includes

[33] Standard errors are about one to two orders of magnitudes smaller than the dispersion across passengers.

Table SA.1. Dyadic Regression: Effects of Compatibility Measures and Time to Departure on Match

α_z	
Compatibility Score	1.774
	(0.035)
Pickup Distance (km)	-0.022
	(0.000)
Dropoff Distance (km)	-0.019
	(0.000)
Departure Time	0.024
Difference $\leq$5 minutes	(0.007)
Departure Time	0.050
Difference $\leq$15 minutes	(0.006)
Passenger Departure	-0.099
Later Than Driver's	(0.007)
α_f, Fare ($)	0.098
	(0.002)
α_{30}	0.015
	(0.008)
α_{20}	0.040
	(0.007)
α_{10}	0.049
	(0.007)
α_x	
Distance 10-30 km	-0.335
	(0.011)
Distance >30 km	-0.779
	(0.022)
Start in Downtown	-0.130
	(0.006)
End in Downtown	-0.085
	(0.006)
Intercept	-0.087
	(0.015)
R^2	0.01
Number of Dyads	2,449,963

Note: The dependent variable is 1 if the dyad is a match and 0 otherwise. All estimates are in percentage point terms (multiplied by 100). We report robust standard errors in parentheses.

Figure SA.2. Passenger Match Probabilities

(a) Match Probability Over Time

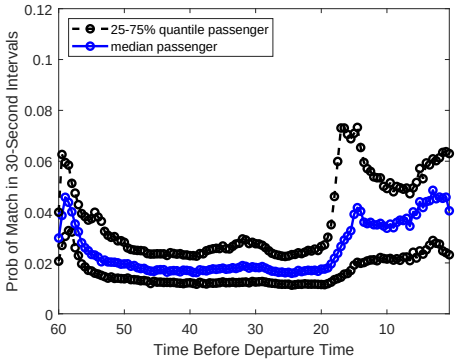

(b) Beliefs Across Passengers

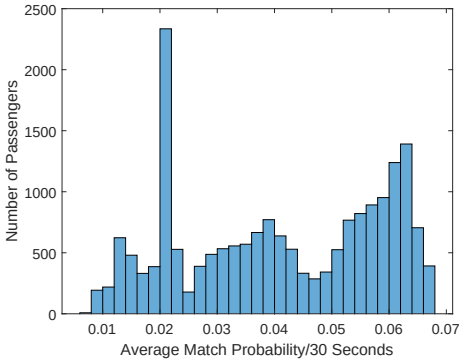

Note: (a) plots the estimated match probabilities as time approaches the departure time. The black lines represent the 25% and 75% quantiles of the match probabilities across passengers and reflect the dispersion of this probability for different passengers, and the blue line represents the median. The differences represent dispersions across passengers. Standard errors are one to two orders of magnitudes smaller than the cross-passenger differences. Panel (b) plots the distribution of the constructed passenger beliefs based on the match probability over time.

1. the waiting passengers that arrive between 4:30 pm and 5:00 pm in data, and

2. a set of simulated passengers that arrive outside this time window.

For each simulated j that arrives outside our data window (i.e., $t_j^0 \notin$ [4:30 pm, 5:00 pm]), we find the period $\mathfrak{t}_j(t)$ that includes t, and then linearly interpolate the mass n_{jt} at t from $n_{j,\mathfrak{t}_j(t)}$ and $n_{j,\mathfrak{t}_j(t)+1}$. Then we randomly and independently include j in the driver's choice set at t with probability n_{jt}. In the simulated likelihood function, we simulate 50 passenger sets for each instance of a driver search, and for each set we independently simulate a set of ν_{ij} for each driver-passenger pair.

SA.5 Driver Value Function and Passenger Waiting Cost Estimates

The estimates of homogeneous parameters are provided in Table SA.2, and the distributions of heterogeneous parameters are in Table SA.3.

SA.6 Driver Move Frequency

We assume that a driver moves at most once every 5 minutes, which corresponds with a search instance during that interval in the data. For each 5-minute interval after arrival, we estimate the probability of a search as a logit function of driver characteristics. Covariates include driver distances (whether the driver distance is less than 10 km, whether it is between 10-30 km) and locations (whether the driver starts in downtown, whether the driver ends in downtown) and a constant. We estimate the move probability separately for each 5-minute intervals up to the last 5 minutes before departure, allowing the probability of search to vary flexibly over time. Each regression's sample consists of drivers that are still in the market at the corresponding time. We set the move probability to be 1 in the last five

Table SA.2. Driver Value Function and Passenger Cost Estimates: Homogeneous Parameters

		Driver	Passenger
Characteristics θ_x, ϑ_x			
	Intercept	-0.09	-0.05
		(0.27)	(0.00)
	Distance 10-30 km	0.93	
		(0.17)	
	Distance>30 km	1.02	
		(0.18)	
	Start in CBD	0.34	-0.01
		(0.11)	(0.00)
	End in CBD	0.38	0.01
		(0.11)	(0.00)
Marginal Value of Waiting			
	$\theta^0_{10}, \vartheta^0_{10}$	1.00	0.00
		(0.06)	(0.00)
	$\theta^0_{20}, \vartheta^0_{20}$	-0.54	0.00
		(0.06)	(0.00)
	$\theta^0_{30}, \vartheta^0_{30}$	0.23	0.00
		(0.06)	(0.00)
	$\theta_{10}, \vartheta_{10}$	-3.60	0.01
		(0.29)	(0.00)
	$\theta_{20}, \vartheta_{20}$	-0.58	0.12
		(0.38)	(0.00)
	$\theta_{30}, \vartheta_{30}$	1.78	0.02
		(0.46)	(0.00)
	$\theta_{60}, \vartheta_{60}$	-2.07	0.17
		(0.55)	(0.00)
	Time Interacted with Characteristics		
	Distance 10-30 km	-0.45	
		(0.23)	
	Distance>30 km	-0.63	
		(0.24)	
	Start in CBD	-0.30	-0.00
		(0.14)	(0.00)
	End in CBD	-0.30	-0.00
		(0.15)	(0.00)

Table SA.3. Driver Value Function and Passenger Cost Estimates: Heterogeneous Parameters

		Driver	Passenger
Component 1			
	θ_k,ϑ_ℓ	-0.09	-0.15
		(0.27)	(0.01)
	$\theta_{10,k}, \vartheta_{10,\ell}$	-3.60	
		(0.29)	
	$\theta_{20,k}, \vartheta_{20,\ell}$	-0.58	
		(0.38)	
	$\theta_{30,k}, \vartheta_{30,\ell}$	1.78	
		(0.46)	
	$\theta_{60,k}, \vartheta_{60,\ell}$	-2.07	0.07
		(0.55)	(0.02)
	Prob	0.53	0.26
		(0.02)	(0.01)
Component 2			
	θ_k,ϑ_ℓ	3.58	-0.05
		(0.39)	(0.00)
	$\theta_{10,k}, \vartheta_{10,\ell}$	-3.90	
		(0.15)	
	$\theta_{20,k}, \vartheta_{20,\ell}$	0.03	
		(0.33)	
	$\theta_{30,k}, \vartheta_{30,\ell}$	3.05	
		(0.59)	
	$\theta_{60,k}, \vartheta_{60,\ell}$	-6.02	0.17
		(0.83)	(0.00)
	Prob	0.47	0.74
		(0.02)	(0.01)

minutes till departure. Similar to Figure SA.2, we plot the the median estimated probability and 25-75% quantiles across drivers in Figure SA.3. In general, the probability increases as time approaches the departure time.

SA.7 Robustness: Waiting Cost

We consider whether the waiting costs depend on when an agent arrives relative to the departure time. Specifically, we include three indicators in the driver value functions and the passenger waiting cost functions. The indicators are whether the arrival time is 10, 20, and 30 minutes before the departure time. The estimated distribution of waiting costs are plotted in Figure SA.4, and they are similar to the main specification in 5.

SB Interviews

Our interviews consist of two waves. The first wave was conducted in the city where our data were collected. The second wave was in Beijing.[34] Nine college student interviewers sent ride requests via the carpooling app. They conducted interviews with their drivers during the trips. The detailed descriptions of the interview process and results are available on the author website.[35]

[34]The change of location was due to the Covid shutdowns.

[35]https://econ-chenyu-yang.github.io/carpooling_interview.pdf

Figure SA.3. Move Arrival Probability

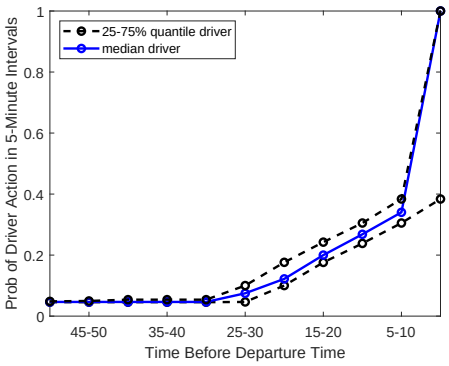

Figure SA.4. Waiting Cost Estimates

(a) Driver

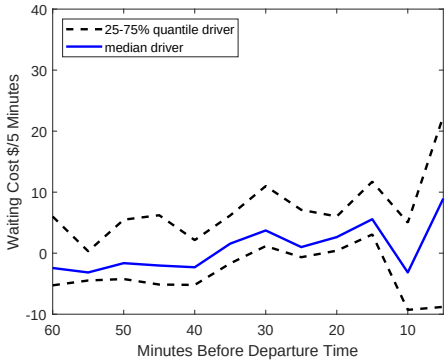

(b) Passenger

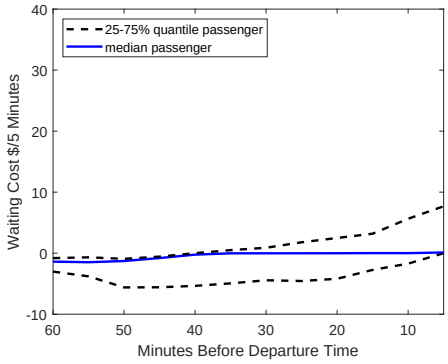

Note: The waiting costs are in units of $/5 minute in 2018 USD. For a given 5-minute interval, points on the black broken lines represent the 25% and 75% quantiles of waiting costs across drivers or passengers. The blue line represents the median costs.

SB.1 Match Quality

We find that the most important factors of match quality are the similarities of routes and departure times. In the first wave of interviews, we asked drivers to list their criteria for matching with a passenger, and 10 out of 12 drivers mentioned route similarity. The second most mentioned criterion is the similarity of departure time (7), followed by passenger rating[36] (5) and whether the passenger offers a tip (1). In the second wave, we further asked drivers to rank the criteria identified in the first wave. Among 22 drivers, 17 ranked route similarity the first, and 20 drivers listed route or time similarity as top 2 priorities. Finally, nearly all drivers were able to discuss route similarity using the compatibility score, where 32 out of 34 drivers could give us numerical thresholds (such as 90%) for whether to accept a passenger in various scenarios in the following section.

SB.2 Driver Values of Waiting

We find some evidence that the value of waiting decreases over time, but less evidence that driver decisions are sensitive to the number of compatible passengers in a driver's choice set. Specifically, we ask the drivers the following set of questions:

1. What is the minimum compatibility score you may accept for a passenger at time t?
2. (First wave) Would you accept a passenger with a compatibility score in the first question immediately at a time $t' < t$? (Second wave) Would you choose a passenger with a lower compatibility score at time $t'' > t$?

We use the first question to help the driver frame the choice problem. In the first wave, t is 5 minutes before the driver would stop searching and leave without a match.[37] There are 4 drivers that would not accept the passenger with a compatibility score in the first question at $t' = t - 10$, and 7 such drivers at $t' = t - 25$. This pattern suggests a higher value of waiting at an earlier time. The evidence is more mixed in the second wave in Beijing. We set t to be 40 minutes before the departure time and $t'' = t + 20$. There are 5 (of 22) drivers that would require a lower compatibility score when the time approaches the departure time, while 3 would have stopped searching. We further asked the rest of the drivers why they would not relax the matching criteria. Drivers pointed to the cost of time in traffic if they chose a passenger with an incompatible route. We do note that traffic in Beijing is substantially worse than in the city of the first wave. In addition, drivers use coarse cutoffs (usually multiples of 10 percentage points) for whether to accept a passenger. It is possible that a 10 percentage point decrease in compatibility score has a much larger negative impact on drivers in Beijing than in our sample city.

We next assess how sensitive driver decisions are to the size of the choice set. Sufficiently sophisticated drivers can, for example, infer that if there are more compatible passengers at a time, the value of waiting is higher because the chance that all such compatible passengers become unavailable in the

[36] The rating is similar to passenger ratings on ride-hailing platforms and scored by drivers. Low ratings may reflect, for example, past disputes with drivers.

[37] Most drivers (8 of 12) would search until their departure time. One driver would stop searching 30 minutes before the departure time. Two would wait past the departure time. One could not give a definitive answer.

next 5 minutes is lower. Such a driver would be more likely to delay the match and wait for a more compatible passenger.

We find that most drivers in both waves are not more likely to wait when there are more than one acceptable passenger. We asked drivers whether they would wait (instead of matching immediately) when there were two or more passengers with minimally acceptable compatibility scores, following the first question above. All 12 driver in the first wave would match immediately. In the second wave, 16 out of 22 drivers would match immediately, and 5 drivers would wait. One driver was unsure about how she would adjust. These results show that the decisions of a large majority of drivers (82%) are not sensitive to the number of acceptable passengers as long as there is one.

SC Driver Value Function and Passenger Waiting Cost Function

We specify the value function as a piece-wise linear function in t:

$$\begin{aligned} V_k(t) \equiv & \mathrm{V}(T_k - t, x_k, \Theta_k) \\ = & \theta_k + \theta_x x_k + \theta_{60,x} \mathbb{1}(T_k - t < 60) \left(1 + \frac{t - T_k}{60}\right) x_k \\ & + \sum_{\tau \in \{10,20,30,60\}} \left\{ \theta_\tau \mathbb{1}(T_k - t < \tau) \left(1 + \frac{t - T_k}{\tau}\right) \right. \\ & \left. + \theta_{\tau,k} \mathbb{1}(T_k - t < \tau) \left(1 + \frac{t - T_k}{\tau}\right) \right\} \\ & + \sum_{\tau \in \{10,20,30\}} \theta^0_\tau \mathbb{1}(T_k - t < \tau). \end{aligned}$$

The unobserved heterogeneity is $\Theta_k = \left\{\theta_k, \{\theta_{\tau,k}\}_{\tau \in \{10,20,30,60\}}\right\}$. Most of the drivers arrive within one hour to the departure time, and we do not include a separate term for $\mathbb{1}(T_k - t < 60)$. We note that inverting the waiting cost requires differentiating the function with respect to t, and the flexible V function is not differentiable on a measure 0 set. We overcome this issue by discretizing time and using numerical derivatives.

The passenger waiting cost function $o_\ell(t)$ has a similar form as V. We specify the cost function as $o_\ell(t) = \mathrm{o}(T_\ell - t, x_\ell, \Theta_\ell)$, replacing the k subscript and parameters θ in the specification of V above with ℓ and ϑ. We also reduce the number of heterogeneous parameters and include $\vartheta_{60,\ell}$ and ϑ_ℓ. We additionally restrict $\vartheta_\tau + \vartheta_{\tau,\ell} > 0$ and $\vartheta^0_\tau > 0$ to ensure that the function increases in t. The hazard rate used in likelihood is calculated via numerical differentiation.

SD Numerical Solution of the Equilibrium in the Empirical Model

We first discuss how we solve the equilibrium in Appendix A.3. Appendix SD.2 describes the expressions of several market level statistics. Appendix SD.3 describes a method to find multiple equilibria. Appendix SD.4 adapts the method to find the optimal waiting values. Appendix SE describes simulating a policy that hides certain passengers from drivers.

SD.1 Solution Procedure

We first simulate driver and passenger types. We assume that matching starts at 4:00 pm, 30 minutes before the start of our sample. We also assume that driver arrival times approximate a Poisson process. We simulate the driver arrival times from 4:00 pm to 6:00 pm, where the inter-arrival time is exponentially distributed with the estimated rate of 77.6 drivers/minute. For each arrival time, we simulate the respective driver's route and departure time based on their empirical distribution. We draw driver heterogeneity parameter (β_k, Θ_k) based on the estimated distribution independently across pairs of 2km-by-2km square regions. The draws are then assigned to the respective drivers based on which squares the trip origins and destinations . We repeat this procedure for passengers, where the arrival times approximate a Poisson process with a rate of 31.77 passengers/minute.

We next solve for driver and passenger choice probabilities and the transitions of the mass. We use $\imath$ and $\jmath$ to driver and passenger types. The simulation uses 6,000 $\imath$s and $4,000$ different $\jmath$s. We use $t_\imath^0, T_\imath, t_\jmath^0$ and $T_\jmath$ to denote the arrival and departure times of drivers and passengers. We discretize the driver time and set the length of a period to be $\Delta^{\text{drv}} = 5$ minutes. Time is discretized more finely on the passenger side and we set each period to be $\Delta^{\text{psg}} = 0.05$ minutes. By choosing $\Delta^{\text{psg}} \ll \Delta^{\text{drv}}$, we reduce the need to break ties should multiple drivers want to match with the same passenger at similar times.[38] We use $m_{\imath\mathfrak{t}}$ and $n_{\jmath\mathfrak{t}}$ to denote driver driver and passenger masses $\mathfrak{t}$ periods after arrival. The maximum number of periods for $\imath$ and $\jmath$ are denoted as $\mathfrak{T}_\imath = \left\lceil \frac{T_\imath - t_i^0}{\Delta^{\text{drv}}} \right\rceil$ and $\mathfrak{T}_\jmath = \left\lceil \frac{T_\jmath - t_\jmath^0}{\Delta^{\text{psg}}} \right\rceil$. Therefore for $\imath$, $\mathfrak{t}$ varies from 1 to $\mathfrak{T}_\imath$, where each $\mathfrak{t}$ represents the $\mathfrak{t}$th 5-minute interval after the arrival. Similarly for each $\jmath$, $\mathfrak{t}$ varies from 1 to $\mathfrak{T}_\jmath$, where each $\mathfrak{t}$ represents the $\mathfrak{t}$th 0.05-minute interval after the arrival.

SD.1.1 Driver

For each $\imath$ and $\mathfrak{t}$, we uniformly randomly select a time point $t(\imath, \mathfrak{t})$ in the 5-minute period $\mathfrak{t}$ as a driver's potential move time. A driver moves with probability $\Lambda_{\imath\mathfrak{t}}$, estimated in Appendix SA.6. We set $\Lambda_{\imath 1} = 1$, i.e., all arriving drivers can choose an action upon arrival. We construct $\imath'$s choice set as the set of $\jmath$ where $t(\imath, \mathfrak{t}) \in \left[t_\jmath^0, T_\jmath\right]$, i.e., any passenger that overlaps with the move time. We use $\mathfrak{S}_{\imath\mathfrak{t}}$ to denote this set of passengers and $|\mathfrak{S}_{\imath\mathfrak{t}}|$ for the number of passengers in this set. We use $n_\jmath(\imath, \mathfrak{t})$ to denote the passenger $\jmath$'s mass in the period that coincides with $t(\imath, \mathfrak{t})$. Given a move, the probability that the driver observes a non-empty set of passengers is

$$p_{\imath\mathfrak{t}} = 1 - \prod_{\jmath \in \mathfrak{S}_{\imath,\mathfrak{t}}} \left(1 - n_\jmath(\imath, \mathfrak{t})\right),$$

where $h_{\imath\jmath\mathfrak{t}} \in [0,1]$ denotes the probability that a passenger $\jmath$ is visible to the driver $\imath$ in the $\mathfrak{t}$th period after $\imath$'s arrival. We take h values as given when solving for an equilibrium. To solve for driver vale functions, we first simulate a $NS \times |\mathfrak{S}_{\imath\mathfrak{t}}|$ matrix of standard normal draws of driver preference for passengers $\nu_{\imath\jmath}^{(ns)}, ns = 1 \ldots NS$. We set $NS = 50$ in our simulation. For each $1 \times |\mathfrak{S}_{\imath\mathfrak{t}}|$ row vector of νs corresponding with the draw ns, we find the highest match value $\overline{u}_{\imath\mathfrak{t}}^{ns}$ among passengers in the set

[38] We note that Δ^{psg} has a different value from that in Appendix SA.3.

$\mathfrak{S}_{\imath\mathfrak{t}}$. Let $\jmath_{\imath\mathfrak{t}}^{ns}$ be the corresponding passenger index. The driver's Bellman equation is

$$V_{\imath\mathfrak{t}} = \Lambda_{\imath\mathfrak{t}}\Bigg(\Upsilon + \Bigg(\frac{1}{NS}\sum_{ns=1}^{NS} n_{\jmath_{\imath\mathfrak{t}}^{ns}}(\imath,\mathfrak{t})\ln\left(1+\exp\left(\overline{u}_{\imath\mathfrak{t}}^{ns}\right)+\exp\left(V_{\imath\mathfrak{t}+1}\right)\right) \tag{SD.1}$$

$$+ (1-p_{\imath\mathfrak{t}})\ln\left(1+\exp\left(V_{\imath\mathfrak{t}+1}\right)\right)\Bigg)\Bigg) + \left(1-\Lambda_{\imath\mathfrak{t}}\right)V_{\imath\mathfrak{t}+1} - c_{\imath\mathfrak{t}}.$$

The waiting cost $c_{\imath,\mathfrak{t}}$ corresponds with the waiting cost over Δ^{drv} in $\imath$'s period $\mathfrak{t}$. We set $V_{\imath\mathfrak{T}_\imath}=0$.

We use the value function to define the choice probabilities. The probability of choosing $\jmath$ in $\mathfrak{t}>1$ conditional on a move and observing $\jmath$ is

$$q_{\imath\jmath\mathfrak{t}} = \frac{1}{NS}\sum_{ns=1}^{NS}\mathbb{1}\left(\jmath=\jmath_{\imath\mathfrak{t}}^{ns}\right)\frac{\exp\left(\overline{u}_{\imath\mathfrak{t}}^{ns}\right)}{1+\exp\left(\overline{u}_{\imath\mathfrak{t}}^{ns}\right)+\exp\left(V_{\imath\mathfrak{t}+1}\right)}. \tag{SD.2}$$

The leave probability is

$$w_{\imath\mathfrak{t}} = \left(\frac{1}{NS}\sum_{ns=1}^{NS}\frac{n_{\jmath_{\imath\mathfrak{t}}^{ns}}(\imath,\mathfrak{t})}{1+\exp\left(\overline{u}_{\imath\mathfrak{t}}^{ns}\right)+\exp\left(V_{\imath\mathfrak{t}+1}\right)} + \frac{1-p_{\imath\mathfrak{t}}}{1+\exp\left(V_{\imath\mathfrak{t}+1}\right)}\right). \tag{SD.3}$$

The mass function is given by

$$m_{\imath\mathfrak{t}+1} = m_{\imath\mathfrak{t}}\left(1-\Lambda_{\imath\mathfrak{t}}\left(\sum_{\jmath\in\mathfrak{S}_{\imath\mathfrak{t}}} q_{\imath\jmath\mathfrak{t}}n_\jmath(\imath,\mathfrak{t}) + w_{\imath\mathfrak{t}}\right)\right), \tag{SD.4}$$

where

$$m_{\imath 1} = \exp\left(V_{\imath 2}\right)\left(\frac{1}{NS}\sum_{ns=1}^{NS}\frac{n_{\jmath_{\imath 1}^{ns}}(\imath,1)}{1+\exp\left(\overline{u}_{\imath 1}^{ns}\right)+\exp\left(V_{\imath 2}\right)} + \frac{1-p_{\imath 1}}{1+\exp\left(V_{\imath 2}\right)}\right). \tag{SD.5}$$

which is the probability of continuing to wait upon arrival.[39]

SD.1.2 Passenger

We first compute the match rate. For each $\jmath$ and $\mathfrak{t}$, we first find the total mass matched with drivers. Let $m_\imath(\jmath,\mathfrak{t})$ denote the mass of driver $\imath$ when its move time falls in the period $\mathfrak{t}$ of the passenger $\jmath$. We set $m_\imath(\jmath,\mathfrak{t})=0$ if no such time exists for $\imath$. We denote the corresponding driver period as $\tilde{\mathfrak{t}}(\jmath,\mathfrak{t})$. The belief is computed as

$$\gamma_\jmath = \frac{1}{\mathfrak{T}_\jmath}\sum_{\mathfrak{t}=1}^{\mathfrak{T}_\jmath}\sum_\imath \Lambda_{\imath\tilde{\mathfrak{t}}(\jmath,\mathfrak{t})}m_\imath(\jmath,\mathfrak{t})\,q_{\imath\jmath\tilde{\mathfrak{t}}(\jmath,\mathfrak{t})}.$$

When we construct the passenger masses for driver estimation, the belief $\gamma_\jmath$ is replaced with the estimated belief in Appendix SA.3.

[39] This procedure assumes that the unit of mass of a driver type k arrives at t_k^0, which approximates an arrival process where the density of driver arrival η_k in Appendix A.3 is highly concentrated near t_k^0.

We next compute the leaving rate. The survival probability is

$$S_{\jmath \mathfrak{t}} = \frac{1}{1 + \exp\left(o_{\jmath \mathfrak{t}}/\gamma_{\jmath} - v_{\jmath}\right)}, \tag{SD.6}$$

where $o_{\jmath \mathfrak{t}}$ and $v_{\jmath}$ are the estimated waiting costs and passenger match value. The waiting cost $o_{\jmath \mathfrak{t}}$ corresponds with the flow waiting cost over Δ^{psg}. The leaving probability is then

$$r_{\jmath \mathfrak{t}} = \frac{S_{\jmath \mathfrak{t}} - S_{\jmath \mathfrak{t}+1}}{S_{\jmath \mathfrak{t}}}. \tag{SD.7}$$

The conditional mass function is then given by

$$n_{\jmath \mathfrak{t}} = n_{\jmath \mathfrak{t}} \cdot \max \left\{ 0, 1 - \sum_{\mathfrak{t}=1}^{\mathfrak{T}_{\jmath}} \sum_{\imath} \Lambda_{\imath \tilde{\mathfrak{t}}(\jmath,\mathfrak{t})} m_{\imath}\left(\jmath, \mathfrak{t}\right) q_{\imath \jmath \tilde{\mathfrak{t}}(\jmath,\mathfrak{t})} - r_{\jmath \mathfrak{t}} \right\}, \tag{SD.8}$$

with $n_{\jmath 1} = S_{\jmath 1}$. The indicator $d_{\jmath} = 1$ indicates that $\jmath$ commits to waiting till departure time $T_{\jmath}$ and $d_{\jmath} = 0$ otherwise.

The solution algorithms iterates over SD.1 through SD.8 till convergence. The input to the algorithm is the initial passenger mass, $n_{\jmath \mathfrak{t}}, \mathfrak{t} = 1, \ldots, \mathfrak{T}_{\jmath}$ for each simulated $\jmath$. We compute these initial masses using mass transition functions with estimated passenger exit rates. These exit rates are estimated using the same logit functions in Appendix SA.3 but with exits (by matching or leaving without a match) as the outcome. We can also change these initial masses to explore the multiplicity of equilibria. We discuss our approach in Appendix SD.3.

SD.2 Equilibrium Quantities

We provide expressions for aggregate equilibrium outcomes below. Let

$$\begin{aligned}
\mathcal{I}_{\imath} &= \mathbb{1}\left(\text{4:30 pm} \leq t_{\imath}^{0} < \text{5:00 pm}\right) \\
\mathcal{I}_{\jmath} &= \mathbb{1}\left(\text{4:30 pm} \leq t_{\jmath}^{0} < \text{5:00 pm}\right) \\
\widetilde{\mathcal{I}}_{\imath} &= \mathbb{1}\left(\text{5:00 pm} \leq T_{\imath} < \text{5:20 pm}\right)
\end{aligned}$$

1. Number of matches among passengers that arrive between 4:30 pm and 5:00 pm,

$$\sum_{\jmath} \sum_{\mathfrak{t}=1}^{\mathfrak{T}_{\jmath}} \sum_{\imath} \Lambda_{\imath \tilde{\mathfrak{t}}(\jmath,\mathfrak{t})} m_{\imath}\left(\jmath, \mathfrak{t}\right) q_{\imath \jmath \tilde{\mathfrak{t}}(\jmath,\mathfrak{t})} n_{\jmath \mathfrak{t}} \mathcal{I}_{\jmath}.$$

2. Total revenue from passengers that arrive between 4:30 pm and 5:00 pm,

$$\sum_{\jmath} \sum_{\mathfrak{t}=1}^{\mathfrak{T}_{\jmath}} \sum_{\imath} f_{\jmath} \Lambda_{\imath \tilde{\mathfrak{t}}(\jmath,\mathfrak{t})} m_{\imath}\left(\jmath, \mathfrak{t}\right) q_{\imath \jmath \tilde{\mathfrak{t}}(\jmath,\mathfrak{t})} n_{\jmath \mathfrak{t}} \mathcal{I}_{\jmath}.$$

3. Average surplus
$$\frac{\sum_\imath V_{\imath 1}\mathcal{I}_\imath + \sum_\jmath W_\jmath \mathcal{I}_\jmath}{\sum_\imath \mathcal{I}_\imath + \sum_\jmath \mathcal{I}_\jmath},$$
where $W_\jmath$ is the simulated passenger value of $\jmath$ based on (2) if not subject to the patient policy, and (A.12) otherwise. Specifically, we draw $\widetilde{NS} = 100$ logistic shocks for ξ_j. For each shock $\widetilde{ns} = 1, \ldots, \widetilde{NS}$, we first compute the optimal leaving time $\mathfrak{t}_\jmath^{\star\widetilde{ns}}$ as the minimum of $\mathfrak{T}_j$ and $\mathfrak{t}$ that satisfies
$$o_\jmath(\mathfrak{t}) < \gamma_\jmath\left(\zeta_x x_\jmath - \zeta_f f_\jmath + \zeta^{\widetilde{ns}}\right) < o_\jmath(\mathfrak{t}+1).$$
We then compute the value function as
$$W_\jmath = \frac{1}{\widetilde{NS}}\sum_{\widetilde{ns}=1}^{\widetilde{NS}}\left(\begin{array}{l}(1-d_\jmath)\sum_{\mathfrak{t}=1}^{t_\jmath^{\star\widetilde{ns}}}\gamma_\jmath\left(\zeta_x x_\jmath - \zeta_f f_\jmath + \zeta^{\widetilde{ns}} - o_\jmath(\mathfrak{t})\right)(1-\gamma_\jmath)^{\mathfrak{t}-1} \\ +d_\jmath\sum_{\mathfrak{t}=1}^{\mathfrak{T}_\jmath}\gamma_\jmath\left(\zeta_x x_\jmath - \zeta_f f_\jmath + \zeta^{\widetilde{ns}} - o_\jmath(\mathfrak{t})\right)(1-\gamma_\jmath)^{\mathfrak{t}-1}\end{array}\right),$$
where $d_\jmath = 0$ if not subject to the patient policy and 1 otherwise.

4. Drivers
   (a) Among drivers with departure times between 5:00 pm and 5:20 pm, the percentage of drivers who decide to wait after arrival,
   $$\frac{\sum_\imath m_{\imath 1}\widetilde{\mathcal{I}}_\imath}{\sum_\imath \widetilde{\mathcal{I}}_\imath}.$$
   (b) The search duration conditional on waiting after arrival,
   $$\frac{\sum_\imath \sum_{\mathfrak{t}=1}^{\mathfrak{T}_\imath} m_{\imath\mathfrak{t}}(\mathfrak{t}-1)\Delta^{\mathrm{drv}}\widetilde{\mathcal{I}}_\imath}{\sum_\imath \widetilde{\mathcal{I}}_\imath}.$$
   (c) The search duration conditional on a match,
   $$\frac{\sum_\imath \sum_{\mathfrak{t}=1}^{\mathfrak{T}_\imath}\sum_\jmath \Lambda_{\imath\mathfrak{t}} m_{\imath\mathfrak{t}} q_{\imath\jmath\mathfrak{t}} n_\jmath(\imath,\mathfrak{t})(\mathfrak{t}-1)\Delta^{\mathrm{drv}}\widetilde{\mathcal{I}}_\jmath}{\sum_\imath \sum_{\mathfrak{t}=1}^{\mathfrak{T}_\imath}\sum_\jmath \Lambda_{\imath\mathfrak{t}} m_{\imath\mathfrak{t}} q_{\imath\jmath\mathfrak{t}} n_\jmath(\imath,\mathfrak{t})\widetilde{\mathcal{I}}_\jmath}.$$
   (d) The average surplus is $\dfrac{1}{\sum_\imath \widetilde{\mathcal{I}}_\imath}\sum_\imath V_\imath \widetilde{\mathcal{I}}_\imath$.

5. For passengers, the percentage that waits, the conditional search duration and the average surplus are defined analogously to the driver's. The search duration conditional on matching is
$$\frac{\sum_\jmath \sum_{\mathfrak{t}=1}^{\mathfrak{T}_\jmath}\sum_\imath \Lambda_{\imath\tilde{\mathfrak{t}}(\jmath,\mathfrak{t})} m_\imath(\jmath,\mathfrak{t})\, q_{\imath\jmath\tilde{\mathfrak{t}}(\jmath,\mathfrak{t})} n_{\jmath\mathfrak{t}}(\mathfrak{t}-1)\Delta^{\mathrm{psg}}\mathcal{I}_\jmath}{\sum_\jmath \sum_{\mathfrak{t}=1}^{\mathfrak{T}_\jmath}\sum_\imath \Lambda_{\imath\tilde{\mathfrak{t}}(\jmath,\mathfrak{t})} m_\imath(\jmath,\mathfrak{t})\, q_{\imath\jmath\tilde{\mathfrak{t}}(\jmath,\mathfrak{t})} n_{\jmath\mathfrak{t}}\mathcal{I}_\jmath}.$$

SD.3 Search for Multiple Equilibria

The input to our algorithm is the vector of initial passenger masses, $n_{\jmath\mathfrak{t}}, \mathfrak{t} = 1, \ldots, \mathfrak{T}_\jmath$ for each simulated $\jmath$. While we use the initial values estimated from their implied empirical distributions in data for our main results, we can also vary the initial input to explore the multiplicity of the equilibria. Choosing the initial $n_{\jmath\mathfrak{t}}$ for each passenger-period is computationally infeasible. We instead group passengers and assign the same $n_{\jmath\mathfrak{t}}$ to those in the same group. The grouping is based on the observed passenger characteristics.

1. Route popularity. We measure the popularity of a trip using the number of passenger requests that travel to and from the same pair of 2 km-by-2 km squares as the route over all days in our sample. The motivation is that drivers across these groups differ in the expected number of compatible passengers and therefore the effects of additional waiting. Similarly, passengers across different groups face different distributions of drivers and should differ in their assessments of the values of waiting. An agent is in one of the popularity groups $\mathcal{G}_1^{\text{pop}}, \ldots, \mathcal{G}_5^{\text{pop}}$ $[0, 1]$, $(1, 2]$, $(2, 5]$, $(5, 8]$, $(8, \infty]$.

2. Time. We also classify the time periods of each agent based on the corresponding time-to-departure $T_\jmath - \Delta^{\text{psg}}\mathfrak{t}$, which may be in one of groups (in unit of minutes) $\mathcal{G}_1^{\text{dept}}, \ldots, \mathcal{G}_5^{\text{dept}}$: $[0, 5]$, $(5, 7.5]$, $(7.5, 10]$, $(10, 20]$ and $(20, \infty]$.

The algorithm chooses $n_{11}^{\text{psg}}, n_{12}^{\text{psg}}, \ldots, n_{55}^{\text{psg}}$ for each combination of $\mathcal{G}_1^{\text{pop}} \ldots$ and $\mathcal{G}_1^{\text{dept}} \ldots$. The weights are then assigned to the corresponding $n_{\jmath\mathfrak{t}}$ as the initial passenger masses. For each set of initial masses, we use the algorithm in SD.1 to compute the corresponding equilibrium solution and the number of matches based on the formula in SD.2.

We choose these initial values to maximize or minimize the number of equilibrium matches through the surrogate minimizer in MATLAB. In our experiments with many starting values, we find multiple equilibria, but they are quantitatively similar.[40] For example, the maximum number of matches across the equilibria we find is 405.86, relative to the baseline 405.82, which are based on initial passenger masses estimated from data (Appendix SD.1).[41]

SD.4 Optimal Waiting Values

We choose $\widetilde{V}_k(t)$ to maximize the total surplus, while allowing the passengers to endogenously adjust their optimal leaving times. Similar to the problem of finding multiple equilibria, directly choosing $\widetilde{V}_k(t)$ is computationally infeasible. We instead adopt a similar dimension reduction technique. Specifically, we can construct analogous driver groups for each combination of $\mathcal{G}^{\text{pop}}$ and $\mathcal{G}^{\text{dept}}$. The algorithm chooses $\widetilde{V}_{11}, \widetilde{V}_{12}, \ldots, \widetilde{V}_{55}$ and sets the new waiting value to be $V_k(t) + \widetilde{V}_{\mathfrak{g}(k,t)}$, where $V_k(t)$

[40] This exercise does not amount to a complete enumeration of all possible equilibria. Any solution to the set of ordinary differential equations and the maximization problems, collected in Appendix A, is an equilibrium. Given that directly solving the large number of ordinary differential equations is computationally prohibitive, we simplify the problem by focusing on equilibria computable through the iterative procedure in Appendix SD.1. This exercise can alternatively be framed as searching within the refined set of equilibria that are fixed points of the mapping from the space of passenger masses to itself defined by the procedure in Appendix SD.1.

[41] Our convergence criterion is for the difference in driver and passenger masses to be within 10^{-6} between iterations.

is the equilibrium waiting value in the decentralized market, and $\mathfrak{g}(k,t)$ is the corresponding group index for k and time t. The algorithm then computes the resulting equilibrium surplus. We use the surrogate minimizer in MATLAB to choose $\widetilde{V}$s to maximize the total surplus.

SE Selective Visibility

In this section, we introduce a parameter $h_{k\ell} \in [0,1]$, which controls the probability that a type ℓ passenger is visible to a type k driver conditional on this passenger being in the driver's choice set. Recall that one passenger of type ℓ is in the driver choice set with probability $n_{\ell t}$, where $n_{\ell t}$ is the passenger mass at t.

SE.1 Modified Equilibrium Conditions

We first define driver beliefs. The probability of observing a non-empty set for a type k driver is

$$p_k(t) = 1 - \prod_{\ell} \left(1 - h_{k\ell}(t)\, n_\ell(t)\right). \tag{SE.1}$$

For $g_{k\ell}$, if the driver value for matching with a type ℓ passenger is u, then the probability that the driver prefers this passenger to another type ℓ' passenger is $\Phi\left(\frac{u-u_{k\ell'}}{\sigma}\right)$. Therefore the probability that the driver prefers this passenger to any other passenger is

$$g_{k\ell}(u;t) = h_{k\ell}(t) \cdot n_\ell(t) \cdot \prod_{\ell' \neq \ell} \left(h_{k\ell'}(t)\, n_{\ell'}(t) \cdot \Phi\left(\frac{u-u_{k\ell'}}{\sigma}\right) + 1 - h_{k\ell'}(t)\, n_{\ell'}(t)\right), \tag{SE.2}$$

where $1 - h_{k\ell'}(t)\, n_{\ell'}(t)$ is the probability that the type ℓ' passenger is not in the choice set. Hence the density function $g_k(u;t)$ of $G_k(u;t)$ is

$$g_k(u;t) = \frac{\sum_\ell g_{k\ell}(u;t)\, \phi\left(\frac{u-u_{k\ell}}{\sigma}\right)/\sigma}{p_k(t)}, \tag{SE.3}$$

where ϕ is the standard normal density.

For passengers, we define the passenger belief as the average type ℓ match rate (omitting the t argument):

$$\gamma_\ell = \frac{1}{T_\ell - t_\ell^0} \int_{t_\ell^0}^{T_\ell} \sum_{k=1}^{K} \left(\lambda_k m_k h_{k\ell} q_{k\ell} + h_{k\ell}\eta_k q_{k\ell}\right) dt. \tag{SE.4}$$

The equilibrium places three sets of restrictions on $\{V_k, q_{k\ell}, w_k, S_\ell, r_\ell, p_k, g_{k\ell}, G_k, \gamma_\ell, m_k, n_\ell\}$.

1. (Optimality conditions) The driver value functions and choice probabilities are given in (1), (A.1) and (A.2). The passenger leaving rate is given by (A.3).

2. (Consistent beliefs) The driver beliefs $(p_k, g_{k\ell}, G_k)$ are consistent with (SE.1), (SE.2) and (SE.3); the passenger belief of the average match rate is consistent with (SE.4).

3. (Mass transitions) The driver mass $m_k(t)$ is 0 for $t \notin [t_k^0, T_k]$. For $t \in [t_k^0, T_k]$,(omitting the argument of t)

$$\frac{dm_k}{dt} = \eta_k - (\eta_k + \lambda_k m_k) \cdot \left(\sum_\ell h_{k\ell} n_\ell q_{k\ell} + w_k \right), \tag{SE.5}$$

with the boundary condition $m_k(t_k^0) = 0$. For passengers, the mass $n_\ell(t) = 0$ for $t \notin [t_\ell^0, T_\ell]$. For $t \in [t_\ell^0, T_\ell]$,

$$\frac{dn_\ell}{dt} = -n_\ell \left(\sum_k (\lambda_k m_k + \eta_k) h_{k\ell} q_{k\ell} + r_\ell \right), \tag{SE.6}$$

with the boundary condition $n_\ell(t_\ell^0) = S_\ell(t_\ell^0; \gamma_\ell)$.

SE.2 Choose h

There are a large number of driver and passenger types, and we use a similar dimensional reduction technique in Appendix SD.3. For each combination of simulated driver $\imath$ and passenger $\jmath$ in period $\mathfrak{t}$, we classify the combination into groups and choose a common h for each group. The grouping is based on the observed driver and passenger characteristics. We group them first by route popularity and time to departure in Appendix SD.3, and the by the route compatibility:

- Driver-passenger compatibility. We classify each $\imath$-$\jmath$ pair into two groups based on whether compatibility score is greater than 80%, $\mathcal{G}_1^{\text{comp}}, \mathcal{G}_2^{\text{comp}}$.

The algorithm chooses the following sets of parameters

1. Driver route popularity and move time. The algorithm chooses $h_{11}^{\text{drv}}, h_{12}^{\text{drv}}, \ldots, h_{55}^{\text{drv}}$ for each combination of $\mathcal{G}_1^{\text{pop}} \ldots$ and $\mathcal{G}_1^{\text{dept}} \ldots$.

2. Passenger route popularity and time. Similarly, the algorithm chooses $h_{11}^{\text{psg}}, h_{12}^{\text{psg}}, \ldots, h_{55}^{\text{psg}}$.

3. Compatibility. The algorithm chooses h_1^{comp} and h_2^{comp}.

For $h_{\imath\jmath\mathfrak{t}}$, we use $\mathfrak{g}(\imath)$ to denote the popularity group index corresponding with $\imath$, $\mathfrak{g}(\imath, \mathfrak{t})$ to denote the departure time group index corresponding with $\imath$ and the corresponding period $\mathfrak{t}$,$\tilde{\mathfrak{t}}_\jmath(\imath, \mathfrak{t})$ for the passenger $\jmath$'s period when $\imath$ searches in her period $\mathfrak{t}$ and $\jmath$ is a passenger in the choice set, and use $\mathfrak{g}(\imath, \jmath)$ to denote the compatibility group index for $\imath$-$\jmath$ pair. We construct $h_{\imath\jmath\mathfrak{t}}$ as

$$h_{\imath\jmath\mathfrak{t}} = h^{\text{drv}}_{\mathfrak{g}(\imath)\mathfrak{g}(\imath,\mathfrak{t})} \cdot h^{\text{psg}}_{\mathfrak{g}(\jmath)\mathfrak{g}\left(\jmath,\tilde{\mathfrak{t}}_\jmath(\imath,\mathfrak{t})\right)} \cdot h^{\text{comp}}_{\mathfrak{g}(\imath,\jmath)}.$$

In our implementation, the optimization algorithm chooses $h_{11}^{\text{drv}}, h_{12}^{\text{drv}}, \ldots, h_{55}^{\text{drv}}$, $h_{11}^{\text{psg}}, h_{12}^{\text{psg}}, \ldots, h_{55}^{\text{psg}}$ and h_1^{comp} and h_2^{comp} between 0 and 1. For each choice of h, the algorithm computes the equilibrium number of matches and average surplus. Using the surrogate algorithm in MATLAB, we find that $h = 1$ is the maximizer whether the objective is the number of matches or the average surplus. We also find the same result when the compatibility score cutoff for $\mathcal{G}_1^{\text{comp}}$ and $\mathcal{G}_2^{\text{comp}}$ is 85% or 90%.